New technique for high-precision, simultaneous measurements of CH4, N2O and CO2 concentrations, isotopic and elemental ratios of N2, O2 and Ar, and total air content in ice cores by wet extraction

Ikumi Oyabu[1], Kenji Kawamura[1,2,3], Kyotaro Kitamura[1], Remi Dallmayr[4], Akihiro Kitamura[5], Chikako Sawada[6], Jeffrey P. Severinghaus[7], Ross Beaudette[7], Satoshi Sugawara[8], Shigeyuki Ishidoya[9], Dorthe Dahl-Jensen[10,11], Kumiko Goto-Azuma[1,2], Shuji Aoki[12], Takakiyo Nakazawa[12]

1 National Institute of Polar Research, Tokyo 190-8518, Japan
2 Department of Polar Science, The Graduate University of Advanced Studies (SOKENDAI), Tokyo 190-8518, Japan
3 Japan Agency for Marine Science and Technology (JAMSTEC), Yokosuka 237-0061, Japan
4 Alfred Wegener Institute, Am Alten Hafen 26, Bremerhaven 27568, Germany
5 Labosoltech LLC, Tokyo 190-0003, Japan
6 Atmosphere and Ocean Research Institute, University of Tokyo, Tokyo 277-0882, Japan
7 Scripps Institution of Oceanography, University of California San Diego, La Jolla, CA 92093, USA
8 Miyagi University of Education, Sendai 980-0845, Japan
9 National Institute of Advanced Industrial and Technology (AIST), Tsukuba 305-8569, Japan
10 University of Copenhagen, Tagensvej 16, Copenhagen 2100, Denmark
11 University of Manitoba, 66 Chancellors Circle, Winnipeg, Manitoba, R3T 2N2, Canada
12 Tohoku University, Sendai 980-8577, Japan

Correspondence to: Ikumi Oyabu (oyabu.ikumi@nipr.ac.jp)

Abstract. Air in polar ice cores provides various information on past climatic and atmospheric changes. We developed a new method combining wet extraction, gas chromatography and mass spectrometry, for high-precision, simultaneous measurements of eight air components (CH_4, N_2O and CO_2 concentrations, $\delta^{15}N$, $\delta^{18}O$, $\delta O_2/N_2$, $\delta Ar/N_2$ and total air content) from an ice core sample of ~60 g. The ice sample is evacuated for ~2 hours and melted under vacuum, and the released air is continuously transferred into a sample tube at 10 K within 10 minutes. The air is homogenized in the sample tube overnight at room temperature, and split into two aliquots for mass spectrometric and gas chromatographic measurements. Cares are taken to minimize contamination of greenhouse gases with long evacuation time, consumption of oxygen during sample storage by passivation treatment on sample tubes, and fractionation of isotopic ratios with long homogenization time for splitting. Precisions are assessed by analysing standard gases with artificial ice, and by duplicate measurements of the Dome Fuji and NEEM ice cores. The overall reproducibility (one standard deviation) from duplicate ice-core analyses are 3.2 ppb, 2.2 ppb and 3.1 ppm for CH_4, N_2O and CO_2 concentrations, 0.006, 0.010, 0.09 and 0.12 ‰ for $\delta^{15}N$, $\delta^{18}O$, $\delta O_2/N_2$ and $\delta Ar/N_2$, and 0.67 ml_{STP} kg^{-1} for total air content, respectively. Our new method successfully combines the high-precision, small-sample and multiple-species measurements, with a wide range of applications for ice-core paleoenvironmental studies.

1. Introduction

35 Measurements of gas components of polar ice cores have provided valuable information on past climatic, atmospheric and glaciological changes. For example, CH_4, N_2O and CO_2 are important greenhouse gases with natural and anthropogenic variations. CH_4 concentration (defined as a dry air mole fraction in this paper) in deep ice cores is useful for detecting abrupt climate changes and to synchronize age scales of different ice cores (e.g., Blunier and Brook, 2001; Brook et al., 1996; WAIS Divide Project Members, 2015). $\delta^{15}N$ of N_2 and $\delta^{40}Ar$ of Ar provide information on past firn thickness and surface temperature

40 (Huber et al., 2006b; Kobashi et al., 2011; Kobashi et al., 2008; Orsi et al., 2014; Severinghaus and Brook, 1999; Severinghaus et al., 1998). $\delta O_2/N_2$ in some ice cores are proxies for local summer insolation and used to constrain age scales by orbital tuning (Bender, 2002; Kawamura et al., 2007). $\delta^{18}O$ of O_2 records the variations of terrestrial hydrological cycles and used for dating as well as detection of abrupt climate changes (Bazin et al., 2013; Extier et al., 2018; Landais et al., 2010; Seltzer et al., 2017; Severinghaus et al., 2009). Total air content (TAC) is affected by atmospheric pressure, temperature, and firn porosity at bubble

45 close-off (Martinerie et al., 1994; Martinerie et al., 1992) and used for reconstructing ice sheet surface elevation (NEEM community members, 2013) and orbital tuning (Bazin et al., 2013; Lipenkov et al., 2011; Raynaud et al., 2007).

Capabilities of both reducing the sample size and improving the analytical precision of ice core analyses are desired, especially for deep ice cores from low accumulation sites to acquire high-resolution data. For example, the inter-polar difference (IPD)

50 of CH_4 for the Holocene is ~30 – 50 ppb (Beck et al., 2018; Chappellaz et al., 1997; Mitchell et al., 2013), thus analytical uncertainty of a few ppb is required for reconstructing subtle changes in IPD. Uncertainty of < ~0.01 ‰ would be required for $\delta^{18}O$ of O_2 (after correcting gravitational fractionation by $\delta^{15}N$) to detect the changes for Heinrich events (Seltzer et al., 2017; Severinghaus et al., 2009). The smallest amplitude of the local summer insolation variation at the precession band is a few %, and the corresponding amplitude of $\delta O_2/N_2$ may be < 0.5 ‰.

55

High precisions with relatively small samples have already been achieved for some species; ± 2.8 ppb for CH_4 with ~60 g of ice by Oregon State University (OSU) (Mitchell et al., 2013), ± 1.5 ppb for N_2O with ~20 g of ice by Seoul National University (Ryu et al., 2018), and 0.005 ‰ for $\delta^{15}N$ and 0.01 ‰ for $\delta^{18}O$ with ~15 g of ice by Scripps Institution of Oceanography (SIO) (Seltzer et al., 2017; Severinghaus et al., 2009). However, a total of ~100 g of ice and more than one laboratory are required

60 to measure all species. Multiple-species measurements combining gas chromatography (for greenhouse gases) and mass spectrometry (for major gas ratios) have been applied by Tohoku University (Kawamura, 2001; Kawamura et al., 2003, 2007), but with lower precisions than the above-mentioned values and larger samples (> 200 g).

Here, we present a new method developed at National Institute of Polar Research (NIPR) to measure eight air components

65 ($\delta^{15}N$, $\delta^{18}O$, $\delta O_2/N_2$, $\delta Ar/N_2$, concentrations of CH_4, N_2O and CO_2, and TAC) using a 60 g of ice with high precisions. This method has the technical advantages of reducing the sample size without sacrificing precision. It also has the advantage of

Atmospheric
Measurement
Techniques
Discussions

paleoclimatic studies that all the measured species can be compared without any age difference. The method is also desired for very old ice cores from the Antarctic interior, with the resolution for 1.5-million-year ice near bedrock is expected to be on the order of 10 kyr m$_{-1}$ (Parrenin et al., 2017).

70

This paper is structured as follows. Chapter 2 describes the air extraction from ice and the splitting of the extracted air for the analyses by respective instruments. Chapter 3 describes the measurements of the sample air with two gas chromatographs and a mass spectrometer. The system performance and precisions are evaluated by various tests with standard gases (Chapter 4) and comparisons of our data from ~100 ice-core samples (Dome Fuji and NEEM) with published records from other

75   laboratories.

2. Air extraction and split

In order to measure CH_4, N_2O and CO_2 concentrations, isotopic and elemental ratios of N_2, O_2 and Ar, and TAC from one ice sample with high precision, we modified the wet extraction and measurement techniques at Tohoku University (Kawamura et al., 2003; Kawamura et al., 2007; Nakazawa et al., 1993a; Nakazawa et al., 1993b). Briefly, an ice sample of 50 – 70 g is

80   melted under vacuum, and the released air is immediately and cryogenically transferred into a sample tube at < 10 K (cooled with a closed cycle refrigerator) without refreezing the meltwater. It requires a relatively short time (< 10 minutes) for melting ice and transferring extracted air, minimizing contaminations due to degassing from the inner walls of the vessel and line. Also, the pressure over the meltwater is relatively low (~100 – 200 Pa), thus the dissolution of released air in the meltwater is minimal (Kawamura et al., 2003). In comparison, the melt-refreeze method typically requires several tens of minutes to

85   refreeze meltwater (e.g., Brook et al., 2005; Chappellaz et al., 1997; Flückiger et al., 1999), possibly elevates trace gas concentrations in the extracted air by degassing from the inner wall of the vessel, as well as alter the air composition by gas-dependent dissolution in meltwater (at several tens of hPa) and incomplete degassing during refreezing.

The extracted air is homogenized in the sample tube for one night and split into two aliquots for mass spectrometric (MS) and

90   gas chromatographic (GC) measurements. About 20 and 80 % of the sample are used for the MS and GC measurements, respectively.

2.1 Air extraction

A schematic diagram of our extraction system is shown in Fig. 1. The components of the extraction line (tubings, fittings, valves and vessels) are made of electropolished (EP) stainless steel except for traps, which are made of Pyrex glass. The traps

95   1 – 3 have Kovar glass-to-metal transition. It has six inlet ports for stainless-steel vessels, each containing an ice core sample. The vessels and traps 1 – 3 are connected to the line with metal face-seal fittings (Fujikin UJR®, 1/2") using nickel gaskets. Diaphragm metal-seal valves (Fujikin FUDDFM-71G-9.52) are used for all stop valves (V1 – V23). ISO-KF25 flanges are

Atmospheric
Measurement
Techniques
Discussions

Open Access

EGU

attached to both ends of the trap 4 with two-component epoxy adhesive, and Viton o-rings are used for connecting the trap to the line. The vacuum is provided by a turbomolecular pump (Pfeiffer HiPace 80) backed by an oil rotary pump (Edwards).

100 The vessels are made of stainless steel pipe (65A) with Conflat flange (ICF114) with a volume of ~600 cm_3, and the sample tubes are made of 1/4" EP stainless-steel tube with a metal-seal valve (Fujikin FUDDFM-71G-6.35) with a volume of 6.6 cm_3.

After the construction of the extraction line (before actual use), we performed pre-treatment of inner surfaces of all the lines, vessels and sample tubes as follows. Pure O_2 (> 99.999 %) was humidified by bubbling through pure-water in a glass flask sealed with silicone cap at room temperature, and flowed into the lines and vessels heated to 90 – 100 ˚C with heating tapes at

105 a flow rate of ~20 – 50 ml min_{-1} for two weeks to efficiently remove trace organic substances and hydrocarbons. After the treatment, the line and vessels were evacuated at 90 – 100 ˚C by a turbomolecular pump for one week. The same treatment is applied to the sample tubes for air extraction.

For routine air extraction, the sample tubes and extraction line are evacuated overnight to $< 1.3 \times 10_{-4}$ Pa (measured at the

110 head of the turbomolecular pump with an ionization gauge, P3). If no extraction is planned for two days or more (i.e., on weekends and holidays), the sample tubes and extraction line are filled with pure air (> 99.99995%) at ~500 Pa. On the day of air extraction from ice core samples, trap 4 is cooled to -196 ˚C by liquid nitrogen to evacuate further the sample tubes and extraction line ($< 10_{-4}$ Pa). The vessels are brought out from an oven at 50 ˚C and cooled to room temperature in ~30 min, and

115 then brought to the cold room at -20 ˚C for further cooling. Ice core samples of ~90 – 150 g, typically 7- to 12-cm long, are cut out from bulk ice-core samples with a band saw in a cold room at -20 ˚C. The same band saw is used to trim all faces for rough decontamination, removing ~2 – 11 mm from the original surfaces. The inner ~50 – 70 g of ice is used for the air extraction, and the removed outer ice is stored for other measurements (e.g., for multiple analyses in case of measurement failures). The amount of ice may be reduced to ~35 g for all measurements with somewhat lower precisions, and to ~9 g if

120 only MS measurements are conducted (without sample splitting).

As $\delta O_2/N_2$ and $\delta Ar/N_2$ ratios of the Dome Fuji ice core become highly fractionated especially near the surface of ice samples due to diffusive gas loss during ice storage, the surface must sufficiently be removed to precisely measure the air composition (Bereiter et al., 2009; Ikeda-Fukazawa et al., 2005; Kawamura et al., 2007). The gas loss also affects $\delta_{18}O$ and $\delta_{40}Ar$ because

125 it is weakly mass-dependent (Severinghaus et al., 2009). The thickness of required surface removal depends on the storage period, storage temperature and the form of air in ice (bubbles or clathrate-hydrates). On the other hand, it is established that the gas-loss effect is not important for greenhouse gas concentrations because of their large molecular sizes, high natural variability and measurement uncertainties. The fractionation of $\delta O_2/N_2$ is the most problematic among the measured species, thus we tested different thicknesses of surface removal from the first Dome Fuji core stored at -50˚C for 20 years by focusing

130 on $\delta O_2/N_2$. The surface is firstly trimmed with a band saw and secondly by a ceramic knife. The shaving by knife also enables the visual inspection of the ice for any cracks. We found that more than 8 mm should be removed for clathrate-hydrate ice (>

~1400 m) (details are described in section 5.2). The cleaned ice sample is placed in a pre-cooled extraction vessel and sealed with a Conflat flange and copper gasket. The vessels are placed in a dewar vessel that accommodates a copper tube (o.d. = 78 mm, i.d. = 74 mm, height = 135 mm) and a eutectic refrigerant bag (~1000 g, pre-cooled to -50 °C), to keep the ice temperature

135   below -25 °C.

Up to six vessels, thus prepared, are brought to our laboratory room at room temperature. All valves on the extraction line are closed, and the closed-cycle refrigerator is turned on. Then, pure air is introduced from V16 to purge the manifold for vessels, and the vessels are connected to the line. The room air is evacuated from the vessels with the turbomolecular pump. After ~5

140   min when the pressure after two water traps (i.e., without water vapor) is below 10_{-2} Pa, the flanges and connections are leak-tested with a helium leak detector (< 10_{-8} Pa L s_{-1}). Then, pure air is introduced into the vessels and pumped out four times to further remove room air from the vessels. All the vessels are then evacuated for 90 min through the evacuation line (Fig. 1, blue). Typically, four to five samples are simultaneously evacuated. The evacuation is made to remove residual room air from the vessels as well as to sublimate the ice surface for further cleaning of the sample. Then, the vacuum line is switched to

145   sample transfer line (Fig. 1, pink), which is the line for transferring sample air during the extraction, by closing V8, V9, V14 and V17, cooling the traps 2 and 3 to -80 °C with ethanol, and opening V22, V13, V10 and V8. The evacuation continues for another 30 min.

After the evacuation, all vessels, except for one for the first extraction, are isolated by closing V2 – V7. V19 and V21 are

150   opened, and the vessel and line are evacuated for another ~5 min. V22 is closed to stop the evacuation, and the valve of a sample tube is opened to establish the line for sample air transfer. Then, the ice sample is melted by immersing the vessel in a hot water bath (~90 °C) by a few mm from the bottom. The air released from the melting ice is continuously transferred into the sample tube at ~10 K, after passing through two water traps at −80 °C. The first trap has sufficient inner volume to condense a large amount of water vapor, and the second trap contains fine glass tubes for high trapping efficiency. Sample transfer is

155   monitored by a Baratron Gauge (MKS, full scale = 1333 Pa) (P1 in Fig. 1), which measures the sample air pressure in the line without water vapor. The maximum pressure during the transfer is ~100 – 200 Pa. The hot water bath is removed after the completion of ice melting. When the pressure decreases below the detection limit (0.1 Pa), the sample transfer is considered to be complete, and the valve of the tube is closed. Residual pressure in the transfer line is measured using a Convectron Gauge (Granville-Phillips, P2 in Fig. 1) (typically <0.2 mTorr). The time required for melting the ice sample is <~3 minutes, and the

160   total time for the air transfer takes ~10 min (including the ice melting). Finally, the valve of the vessel is closed, and the line is evacuated for ~2 min to decrease the pressure to <10_{-4} Pa (P3).

The pressure of air released from the ice sample in the next vessel during the previous transfer is measured with the Baratron Gauge (P1) by closing V20, V21 and V22 and opening the valve of the vessel (typically <1.0 Pa for the second vessel and ~4

165   Pa for the fifth vessel). This ensures the absence of a leak at the flange and fitting of the vessel. Then, V22 and V21 are opened,

and the line and vessel are evacuated for ~5 min, the ice sample is melted, and the released air is transferred to the next sample tube. We repeat these procedures until all the extractions are completed.

After collecting the air from all prepared samples, the sample tubes are removed from the helium cycle cooler and laid in the laboratory room with ambient temperatures for one night. All the vessels and traps are also disconnected from the line, rinsed with pure water, and placed in ovens at 50°C for drying. Another set of sample tubes and traps are connected to the line and evacuated with the turbomolecular pump (to <10^{-2} Pa), and then the line is checked with a helium leak detector (< 10^{-8} Pa L s^{-1}). After the leak check, all the valves are opened, and the line is evacuated until the next extraction.

2.2 Splitting

A small aliquot of air is separated from the sample tube and transferred to a second tube using the "split line" (Fig. 2) for MS analysis. We employed the general design of the line for noble gas measurements developed at SIO (Bereiter et al., 2018). The split line is made of electropolished stainless steel except for a U-shaped cold trap, which is made of Pyrex glass and connected to the line with bored-through 3/8" UltraTorr® fittings (Swagelok). A diaphragm metal-seal valve (Fujikin FUDDFM-71G-6.35) is placed next to the sample tube (V1) for splitting, and stainless-steel bellows valves (Swagelok SS-8BW or SS-4H) are used for other valves. The vacuum is provided by a turbomolecular pump (Pfeiffer HiPace80) backed by a dry scroll pump. The same pre-treatment with humidified O_2, as applied to the extraction line, is employed for the split line. To minimize the depletion of the $\delta O_2/N_2$ ratio during the sample storage in the tube, a passivation treatment (GoldEP-White®, Nissho Astec Co. Ltd.) is employed, which forms a passive layer of oxidized chromium on the stainless-steel surface (hereafter, this type of tube is called GEPW).

The experimental procedures are as follows. The split line is filled with pure air (> 99.99995%) at ~500 Pa when not in use (e.g., during nights and weekends), and evacuated for more than 30 minutes before the splitting. The GEPW tubes are evacuated overnight. The sample tube containing ice-core air is connected to the split line with a 1/4" UJR® fitting using a silver-plated nickel gasket. The GEPW tube is inserted in a helium cycle cooler at <10 K and connected to an adapter with a VCR® fitting, which is then connected to the split line with a VCO® fitting (Swagelok). The whole line is evacuated for ~30 minutes, during which the pressure decreases to < 3×10^{-5} Pa (measured at the head of a turbomolecular pump with an ionization gauge). After a leak check, V1 is closed, and the valve on the sample tube is opened to expand the sample air into the small volume (1.4 cm^3) between the valves. The time required for equilibration of the air composition in the small volume with the sample tube is > 20 minutes. During this waiting time, the sample air may be fractionated if the temperature gradient exists between the tube and the small volume. To minimize such fractionation, the sample tube and small volume are covered with a sheet of bubble wrap so that air conditioners on the laboratory ceiling do not directly blow against the splitting part. The expanded air is then split by closing the valve of the sample tube. The air in the split volume is transferred to the GEPW tube for 5 minutes, after passing through the cold trap at −196 °C. The sample transfer is monitored by measuring the pressure of

Atmospheric
Measurement
Techniques
Discussions

the line with a Baratoron Gauge (MKS, full scale = 1333 Pa) (P1 in Fig. 2). The GEPW tube is lowered by a few centimeters

200   into the helium cycle cooler when the pressure becomes below 1.0 Pa to improve the trapping efficiency of the gas by exposing fresh metal surface. The air transfer is complete in 5 minutes, and the valve of the GEPW tube is closed. The residual pressure is measured using a Convectron Gauge (Granville-Phillips) (P2 in Fig. 2), and the GEPW tube is disconnected from the line. The GEPW tube is warmed to room temperature and allowed to homogenize the sample air for at least 3 hours before the MS analysis. Sometimes the samples are measured on the following day of the splitting. The air remained in the original sample

205   tube is used for measuring CH_4, CO_2 and N_2O concentrations as well as total air content.

3. Measurements of extracted air

3.1 CH_4, N_2O and CO_2 concentrations

3.1.1 Gas chromatography

After taking the aliquot of air for the mass spectrometer analysis, the air left in the original sample tube was measured for the

210   concentrations of CH_4, CO_2 and N_2O with two gas chromatographs (Agilent 7890A) (Fig. 3). The settings of the GCs are summarized in Table 1. Briefly, CH_4 and CO_2 are measured with one GC (GC1) equipped with two Frame Ionized Detectors (FIDs) (CO_2 is converted to CH_4 by nickel catalyst), and N_2O is measured with another GC (GC2) equipped with an Electron Capture Detector (ECD). We employ capillary columns to obtain high separation and narrow peaks. CH_4 and CO_2 are separated with a GS-Carbon PLOT (Agilent) capillary column (L = 30 m, i.d. = 0.53 mm, film thickness = 3 μm), and N_2O is separated

215   with a HP-PLOT Q (Agilent) column (L = 30 m, i.d. = 0.53 mm, film thickness = 40 μm). We use N_2 (> 99.99995%, Taiyo Nissan corp., Japan) for carrier and make-up gases, and H_2 (> 99.99995%, Taiyo Nissan corp., Japan) for FID for GC1. Hydrocarbon-free air for FID is generated by a zero-air generator (PEAK Scientific, ZA015A). For GC2, we use He carrier (> 99.99995%, Taiyo Nissan corp., Japan) for high separation, and the mixture of Ar and CH_4 (5 %) as makeup gas for high sensitivity. We use two gas purifiers in series (a "Mini Fine Purer" from Osaka Gas Liquid and a "Big Universal Trap" from

220   Agilent) for the carrier, makeup and H_2 gases to ensure their purity. Zero air is further purified with a Hydrocarbon/Moisture Trap (Agilent).

To measure a small amount of sample gas, we use small sample loops (1/16" o.d., 0.5 cm^3, Valco) filled at sub-ambient pressure. Small sample loops are also effective in reducing baseline fluctuations when GC valves are switched. The dead

225   volumes of the inlet, fittings and tubing need to be minimized for filling the loops at sufficient pressure. We achieve the total volume (sample loops and dead volumes) of 3.3 ml by using 1/16" tubing (0.7 mm or 1.0 mm i.d.), a customized metal-seal fitting (VCR) with a small bore (1.5 mm i.d.) for the connection of the sample tube, and a customized bracket with small dead volume for the pressure transducer at the inlet (machined Valco cross fitting). This configuration allows us to fill the sample loops at 400 – 600 for the first injection and 300 – 500 hPa for the second injection, for typical ice-core measurements. The

Atmospheric
Measurement
Techniques
Discussions
Open Access
EGU

230   third injection is necessary if the pressure for the first injection exceeds the range of calibration, or if a gas handling error occurs. To minimize the broadening of CO_2 peak by passing through the nickel catalyst (Agilent G3440-63002), we replaced the 1/4" (o.d.) tube for packing the catalyst with a 1/8" tube. To minimize adsorption/desorption of trace gases on the inner walls of the tubing, we employ VICI® electroformed Ni tubing or mirror-polished stainless-steel tubing (LaboSolTec). Typical chromatograms are shown in Fig. 4.

235

A standard gas measurement at atmospheric pressure is conducted as follows. V8 is set to position 1, V1 is set to OFF, V3 is set to OFF, and V7 is opened to allow the standard gas to flow through the two sample loops at 100 ml min$_{-1}$ for 1.0 min using a mass flow controller (HORIBA STEC, SEC-E40). V7 is closed to stop the gas flow, V3 is set to ON to disconnect the two GCs, and the GC measurements are initiated by switching V1 and V4 to let the carrier gases to flow through the sample loops.

240   In GC1, CH_4 separated by column 1 is detected with the front FID (retention time ~1.8 min). At 1.74 min, V2 is switched to lead CO_2 from column 1 to pass through Ni catalyst (to convert to CH_4) and then to back FID (retention time ~ 2.3 min). Finally, at 4.6 min, V1 and V2 are switched to the original positions. In GC2, immediately after N_2O passes through column 2 (at 1.5 min), V4 is switched to back-flush column 2 to vent H_2O out from the GC during the run. It is important to prevent the accumulation of H_2O in the columns, which may cause unstable baseline during later measurements. N_2O is further

245   separated in column 3, and V5 is switched at 1.95 min to lead N_2O to ECD (air eluting before N_2O is vented to the atmosphere). Finally, at 4.89 min, V5 is switched to the original position. After the run, the sample loops are evacuated to < 0.25 hPa (P1) (Paroscientific Digiquartz® Series 2000, absolute 0.16 MPa full-scale).

For a standard gas measurement at sub-ambient pressure, the sample loops are first evacuated for ~30 min by closing V11,

250   switching V12 and V13 (to connect the sample loops and Dry Pump 1), and turning V3 ON. Then, the standard gas is allowed to flow through Sample Loop 1 by turning V8 to position 1. The flow rate is 100 ml min$_{-1}$ for 1 min, and then 17 ml min$_{-1}$ for 1 min. V3 is turned OFF to isolate the pump and start filling the sample loops. When the pressure (P1) reaches a prescribed value, the flow is stopped by closing V7. Then, 15 sec is allowed to stabilize the pressure and the temperature of the sample loops, and the GC measurements are initiated by switching V1 and subsequently V4 (1 sec after V1) to introduce the carrier

255   gases to the sample loops. The measurement procedures of the GCs are the same as above.

The routine GC calibration and measurement procedures are as follows. We use three standard gases to cover the ranges of greenhouse gas concentrations in the samples (details of our working standard gases are described in the next section and summarized in Table 2). On each day of the measurement, the standard gases in the lines (1/8" tubes) connecting the cylinders

260   and GC inlet are first pumped out for 5 min with a dry pump, and the standard gases are freshly introduced from the cylinders into the lines. The rest of the standard gas handling and measurements are automated with a custom-made software (with LabVIEW). First, the overall stability of the GC system is assessed by measuring the three standard gases three times at atmospheric pressure. For each standard gas, the peak areas of three consecutive measurements must agree within 1 % to

proceed. The linearities of the detector responses are also checked by comparing the middle standard gas concentrations

265 calculated from linear interpolation of the concentration-area relationships of high and low standard gases with the original values. The typical differences are +1.1±1.7 ppb for CH_4, -0.3±0.2 ppm for CO_2, and +2.3±1.2 ppb for N_2O. Then, each of the three standard gases is measured at three sub-ambient pressures (i.e., nine measurements in total) to construct calibration curves for the ice-core measurements. Typical pressures are 300, 450 and 600 hPa to cover the pressure range for two injections of sample air from ~60 g of ice.

270

After all the standard gas measurements, a sample tube is connected to the GC inlet by VCR, V8 is set to position 4, V10 is switched ON to evacuate the inlet with a turbomolecular pump for ~20 sec, and the VCR connection is leak-checked with P2 (JTEKT® PMS-5M-2 pressure transducer). The inlet and two sample loops are then evacuated via V10 and V3, respectively, for 15 min to < 0.25 hPa, V10 is closed, the sample gas is expanded into the inlet by opening the stop valve on the sample

275 tube, and the controlling software is started. Three seconds later, the two sample loops are connected and isolated from the vacuum line (V3 OFF), and the sample air is expanded into the sample loops (V8 position 3). The rest of the GC measurement sequences are the same as the standard gas measurements. After the measurement of a sample, the sample loops are evacuated by switching V3 for ~2 min (P1 < 0.25 hPa), and the second measurement is initiated automatically. After the end of the second measurement, the sample tube is replaced with the next one.

280

After measuring all samples, the standard gases are measured again at the sub-ambient pressures to account for the drifts of GC signals during the sample measurements. The areas of the standard gases before and after the sample measurements were linearly interpolated to the time of the sample measurements for calculating the sample concentrations, assuming that the drift is linear with time.

285

The concentration of greenhouse gas in the sample air is determined as follows. First, the peak areas of the three standard gases at the sample pressure (in the sample loop) are calculated by:

$$A_{St,n,P} = a_n P^2 + b_n P + c_n, \tag{1}$$

where $A_{St,n,P}$ is peak area of standard gas n (= 1 to 3) calculated for the sample pressure (P), and a_n, b_n and c_n are coefficients

290 obtained by second-order polynomial fit to the peak area versus pressure from the calibration measurements. Then, the greenhouse gas concentration in the sample is obtained by:

$$C = dA^2 + eA + f, \tag{2}$$

where C is concentration, A is sample peak area, and d, e and f are coefficients obtained by the second-order polynomial fit to the standard gas concentrations versus $A_{St,n,P}$ (n = 1 to 3). Each sample air is measured at least twice, and the mean values are

295 used.

Atmospheric
Measurement
Techniques
Discussions

3.1.2 Standard gases

The CH_4, N_2O and CO_2 concentrations are determined against Tohoku University (TU) scales, which are based on gravimetrically prepared primary standard gases (Aoki et al., 1992; Tanaka et al., 1983). Uncertainties of the TU primary standards are $< \pm 0.2$, 0.2 and 0.03% for CH_4, N_2O and CO_2 concentrations, respectively (Aoki et al. (1992) for CH_4, Ishijima

300   et al. (2001) for N_2O and Tanaka et al. (1987) for CO_2). The ice-core standard gases are calibrated using the primary standard gases manufactured in 2008 for CH_4 (300.1 – 2799.1 ppb) and CO_2 (200.13 – 449.72 ppm), and those made in 1991 for N_2O (100.0 – 400.1 ppb). Working standard gases at NIPR contain CH_4, N_2O and CO_2 in purified air in 47-L aluminum cylinders (Taiyo Nissan corp., Japan), whose concentrations were calibrated at Tohoku University using their working standard gases named '2007-Ice-Work' (with 25 measurements for each cylinder). We have five working standard gases (named STD 1 – 5)

305   with different concentrations covering from preindustrial Holocene to glacial maxima (Table 2). Two additional cylinders (STD-A and B) are prepared and calibrated against the NIPR working standard gases at NIPR and used for various tests. Uncertainty of CH_4, N_2O and CO_2 concentrations of the NIPR working standards are $< \pm 0.6$ ppb, ± 0.3 ppb and ± 0.02 ppm, respectively (one standard error of the mean).

310   For modern atmospheric concentration levels, the TU scales are in agreement with the NOAA/WMO scales within ~2 ppb for CH_4, ~0.3 ppm for CO_2, and ~0.5 ppb for N_2O as reported in WMO/IAEA Round Robin Comparison Experiment (Dlugokencky, 2005; Tsuboi et al., 2017) (https://www.esrl.noaa.gov/gmd/ccgg/wmorr/index.html). However, at lower concentration levels, inter-calibration between TU and NOAA scales have not been conducted. For CH_4 and N_2O, we discuss the consistency of calibration scales by comparing our ice-core data with those from other laboratories (see section 5.1).

315   ### 3.2 Mass spectrometry for isotopic and elemental ratios of N_2, O_2 and Ar

Isotopic and elemental ratios ($\delta^{15}N/^{14}N$ of N_2, $\delta^{18}O/^{16}O$ of O_2, $\delta O_2/N_2$ and $\delta Ar/N_2$) are analysed on a dual inlet mass spectrometer (Thermo Fisher Scientific, Delta V) with 9 Faraday cups and amplifiers to simultaneously collect ion beams of molecular masses 28, 29, 32, 33, 34, 36, 38, 40 and 44. The registers, typical beam intensities and other MS settings are given in Table 3. While we collect raw data from all of these cups, we do not use the signals of masses 33, 36 and 38 in this paper

320   because high precisions for isotopic ratios with these masses (including appropriate corrections for interference and nonlinearity in the mass spectrometer) are not established. To achieve high precision, we control the temperature around the mass spectrometer (especially around the inlet) by isolating the mass spectrometer from the room-air temperature fluctuation with plastic sheets and introducing temperature-controlled air generated by an air conditioner (Orion PAP03B) into the booth. Two large (~45 cm diameter) and a small (~20 cm diameter) fans in the booth vigorously mix the air to maintain the

325   temperature around the inlet at 25.7 ± 0.3 °C all year round.

Atmospheric
Measurement
Techniques
Discussions

3.2.1 Measurement procedures

Our reference gas is commercially available purified air (>99.9999 %, Taiyo Nissan Co.) in a 47-L cylinder filled in 3-liter
electropolished stainless-steel containers (hereafter reference cans), each with two bellows-seal valves (Swagelok SS-4H)
creating small pipette volume (1.3 cm$_3$) at the exit. The inner surface of the can is preconditioned by humidified O_2 at > 120
330   °C as for the extraction line. The reference can attached to the standard side is rarely disconnected.

Our mass spectrometry largely follows Severinghaus et al. (2009). Prior to the daily sample measurements, a reference can is
connected to the sample port of Delta V using VCO® fitting (typically on the prior evening to stabilize the can's temperature),
and the ports and pipets are evacuated. The MS valves leading to the reference cans are closed, and both bellows are evacuated
335   for 5 min. Then, the MS valves to the inlet ports are opened to check leak by an ion gauge, and all bellows and lines are further
evacuated for 5 min. On both sides, the reference gas is introduced into the pipette of the can by closing the valve at the MS
side and opening the other valve, and they are equilibrated for 10 min. The pipette volumes are disconnected from the cans,
and the aliquots are expanded into the bellows and equilibrated for 10 min. Then, the bellows are isolated from the inlet and
compressed to reach ~30 mbar. The initial pressure in the fully expanded bellows is ~28 mbar from a freshly filled can. The
340   reference can is replaced by a new one when the initial pressure decreases to ~18 mbar.

The reference gas from the sample port is measured against the standard side ("can versus can") for 4 blocks to check the
standard deviations. Before each block, the acceleration voltage is optimized by centering the mass 40 peak, the background
is measured after a 120-sec idle time, and the pressures are adjusted to 5000 ± 50 mV for mass 28 (3 × 10$_8$ Ω), automatically
345   with the ISODAT software. The idle time and integration time are 10 seconds and 16 seconds, respectively. Each block consists
of 17 changeover cycles, but the first cycle is discarded and only the latter 16 values are used. After running the 4 blocks, two
blocks are run by imbalancing the sample pressure by ± 10 % against the standard side for obtaining pressure imbalance
sensitivity (see below).

350   The GEPW tube containing the sample air is connected to the sample port, and the sample port is evacuated during the previous
measurement. The procedure of the sample measurement is the same as the "can vs. can" measurement, except that the sample
expansion into the bellow is made in one step by simply opening the tube valve. We run two blocks for each sample to obtain
a total of 32 cycles. Typical standard deviations in 1 block (16 cycles) are 0.013, 0.029, 0.010 and 0.017 ‰ for $\delta^{15}N$, $\delta^{18}O$,
$\delta O_2/N_2$ and $\delta Ar/N_2$, respectively.

355   ### 3.2.2 Pressure imbalance and chemical slope corrections

The ratios of ion currents of different masses are slightly sensitive to the pressure in the ion source, thus a correction is applied
with an established procedure (Severinghaus et al., 2003). The pressure imbalance sensitivity (PIS) is a slope of δ values

Atmospheric
Measurement
Techniques
Discussions

against differences in beam intensity ($\Delta P = (I_{sa}/I_{st} -1) \times 1000$ where I is the mean beam intensity in one block), which is determined by measuring the reference gas at the sample side at three pressures (at $\Delta P = 0$, +100 and -100 ‰). The PIS is

360 measured every day and used for correcting the sample values measured on the same day by:

$$\delta_{pressure\ corrected} = \delta_{measured} - (PIS)\ \Delta P. \tag{3}$$

The PIS gradually changes over several weeks, and they shift after a filament replacement.

Relative ionization efficiencies of gas are also sensitive to variations in the mixing ratio of the gas in total air (the sensitivity

365 is called "chemical slope") (Severinghaus et al., 2003). The chemical slopes are determined from the measurements of the reference gas added by pure O_2 (+10, +20 and +30 % of original O_2 amount) for $\delta^{15}N$, and pure N_2 (+10, +20 and +30% of original N_2 amount) for $\delta^{18}O$. The correction is made by:

$$\delta^{15}N_{slope\ corrected} = \delta^{15}N_{pressure\ corrected} - [CS1] \times \delta O_2/N_{2measured} \tag{4}$$

$$\delta^{18}O_{slope\ corrected} = \delta^{18}O_{pressure\ corrected} - [CS2] \times \delta N_2/O_{2measured} \tag{5}$$

370

where CS1 and CS2 are chemical slopes for $\delta^{15}N$ and $\delta^{18}O$, respectively. The chemical slopes are fairly stable, thus are measured only a few times per year. The typical values of CS1 and CS2 are 0.0005 ‰/‰ and 0.0018 ‰/‰, respectively.

The final normalization against the modern atmosphere (the ultimate standard gas for ice cores by definition) requires through

375 investigation of the stability of reference gases and the atmospheric ratios, which we discuss in section 4.2.

3.3 Total air content

Total air content (TAC) is the amount of occluded air in a unit mass of ice (ml_{STP} kg-1) (Martinerie et al., 1992). In our system, TAC is calculated from:

$$TAC = \frac{P}{1013.25} \cdot \frac{(V_a+V_c)\cdot(V_a+V_b)}{V_a} \cdot \frac{273.15}{T} \cdot \frac{1}{m}, \tag{6}$$

380 where P is pressure in the sample loops upon first expansion, T is air temperature near GC, m is mass of ice sample (measured with an electronic balance, SARTORIUS CP4202S), and V_a, V_b and V_c are the volume of the sample tube, the volume of the pipette at the split line, and the combined volume of GC inlet and sample loops, respectively.

V_a and V_b were determined manometrically against a known volume (118.7 cm3) with a pressure gauge (Paroscientific

385 Digiquartz® Model 745-100A, absolute 0.69 MPa full-scale). The whole apparatus is first evacuated, the air is introduced from a cylinder into the glass flask at about atmospheric pressure. The air is expanded into the manifold, pipette, and tube, and the pressure measured at each step is used to calculate the volumes by the ideal gas law. The expansion and recording are repeated 10 times, and they are averaged.

Atmospheric
Measurement
Techniques
Discussions

390　Similarly, V_c was determined manometrically for each sample tube (~6.6 cm3), which was attached to the GC inlet. N2 or air in a sample tube at a known pressure was expanded into the evacuated GC inlet and sample loops, and the pressure was recorded (valve on the sample tube is kept open). The expansions/evacuations were repeated a few times, and the gas in the sample tube was re-filled. The whole procedures were repeated a few times to obtain a total of 12 measurements for each tube.

395　The calibration of the volumes V_a, V_b and V_c must be made for individual sample tubes because the volumes in the valves and end connections are slightly different from each other (V_a, V_b and V_c are different by up to 0.8 %, 0.6% and 0.5%, respectively, between the tubes). Average V_a, V_b and V_c are 6.6 cm3, 1.4 cm3 and 3.4 cm3, respectively. The standard error of the mean for the 10 – 12 measurements of V_a, V_b and V_c are 0.04 %, 0.10 % and 0.04 %, respectively. By propagating these values and the uncertainties of temperature (assumed to be 1 K), pressure (assumed to be 16 Pa) and ice mass (assumed to be 0.1 g), 1σ

400　uncertainty of TAC is estimated to be 0.5 mlSTP kg-1.

4. Evaluation of system performance using standard gas and atmosphere

During air extraction, splitting and analyses, alteration of air composition may occur for various reasons, such as gas dissolution or chemical reaction in the meltwater, degassing from inner surfaces of vessel and line, and diffusive fractionations of isotopic ratios. Below, we evaluate the performance of the tubes, apparatus and instruments by various tests and controlled

405　measurements (mimicking ice-core analyses with standard gas and gas-free ice).

4.1 CH4, N2O and CO2 concentrations

4.1.1 Tube storing test

We evaluate the concentration changes during gas storage in the sample tubes and test tubes (used for injecting standard gas to the apparatus, with metal-seal valves at both ends), by filling standard gas from a cylinder (STD-A) into evacuated tubes,

410　and measuring the sample tubes on the following day and the test tubes on the same day. The changes in CH4, N2O and CO2 concentrations thus obtained are insignificant with respect to the measurement precisions for both the sample tubes (+0.8±2.1 ppb, +1.3±2.1 ppb and +0.1±1.1 ppm, respectively, with n = 25) and test tubes (+0.7±2.2 ppb, +0.9±1.0 ppb and ⁻0.2±0.1 ppm, respectively, with n = 17) (Table 4). The excellent results of the storing tests are attributable to the passivation treatment of the tubes and the use of valves with clean inner surfaces (Fujikin metal diaphragm valves). We note from our earlier

415　experience that CH4 is produced by up to several ppb by opening and closing metal bellows valves (Swagelok SS-4H) if they become old (after several hundred operations), and that CO2 concentration increases by up to ~10 ppm if the passivation treatment is insufficient.

Atmospheric
Measurement
Techniques
Discussions

4.1.2 Standard gas transfer test

Gas-free ice for tests is made from ultra-pure water in a stainless-steel vessel (~1800 cm3) sealed with a Conflat blank flange.
420   The water is boiled for 20 – 30 min with an open outlet port on the flange, and cooled to room temperature after closing the outlet, and then put in a freezer at -20 ˚C. The side of the vessel is surrounded by insulation so that the water is frozen from the bottom over a few days. The ice is removed from the vessel, and ice with visible cracks and bubbles are removed (more than half of the ice).

425   Standard gas from a cylinder is flushed through a pre-evacuated line and test tube (volume is 3 or 5 cm3) at 50 ml min-1 for 5 min, and sampled at atmospheric pressure after ceasing the flow by closing an upstream valve. The relatively low flow rate for flushing prevents thermal fractionation of the gas due to adiabatic expansion at the pressure regulator (important for isotopic analyses), and the pre-evacuation and >200 ml of total flow ensure clean sampling.

430   The test tube with standard gas and vessel with ~50 g of gas-free ice are attached to the extraction line, and the vessel is evacuated for 120 min. The ice is melted while the vessel is evacuated (for 15 min) to remove any air degassed from the melt. We also use ice-core melt instead of gas-free ice melt for the blank test. In this case, the vessel with ice-core melt is evacuated for 30 min after a sample extraction to pump out any residual air. Then, the standard gas from the test tube is slowly injected into the extraction system and transferred continuously over the gas-free water into a sample tube, maintaining the pressure
435   similar to that of ice-core extraction.

The standard gas thus transferred to the sample tubes are measured on the following day, after handling it with the split line (see below for the results of isotopic analyses). No significant changes in CH_4, N_2O and CO_2 concentrations are observed with respect to the mean values of the test tubes' storing tests (+0.8±2.7 ppb -0.1±1.7 ppb and +1.3±0.7 ppm, Table 4). Based on
440   the above results, we apply no corrections for CH_4, N_2O and CO_2 concentrations.

4.2 Isotopic and elemental ratios of N_2, O_2 and Ar

4.2.1 Storing test of GEPW tubes

To evaluate the possible effect of gas storage in the GEPW tubes for one day, the reference gas was transferred to the tubes using the split line and measured the following day, and the results were compared with those measured on the same day. They
445   are identical within the measurement uncertainties for all ratios (-0.002 ± 0.003 ‰ for $\delta^{15}N$, -0.002 ± 0.010 ‰ for $\delta^{18}O$, -0.012 ± 0.056 ‰ for $\delta O_2/N_2$, -0.013 ± 0.042 ‰ for $\delta Ar/N_2$, with n=14), thus no corrections are applied for the storage duration in the GEPW tubes.

14

4.2.2 Standard gas transfer test

The standard gas filled in a test tube was transferred to a sample tube with the extraction line and gas-free water (the same
450   experiment as in section 4.1.2), and an aliquot was taken with the split line and transferred to a GEPW tube as the ice-core
analyses (Fig. 5). On the other hand, the same standard gas filled in the same test tube was attached directly to the split line,
and its aliquot was transferred to a GEPW tube, skipping the extraction line and overnight storage (Fig. 5). Comparison of the
measured values from these two experiments gives the changes in the isotopic and elemental ratios during the ice-core air
extraction and overnight storage, denoted as $\Delta\delta_{extraction}$. The values of $\Delta\delta_{extraction}$ are -0.005 ± 0.001, -0.003 ± 0.002 and -0.102
455   ± 0.011 for $\delta^{15}N$, $\delta^{18}O$ and $\delta Ar/N_2$, respectively (errors are standard error, n > 100). The signs of changes are negative for all
gases, which may suggest a slightly less effective transfer of heavier isotopes with our extraction line. Based on these results,
we employ the above values for $\delta^{15}N$ and $\delta Ar/N_2$ as constant corrections, and no correction for $\delta^{18}O$, for the ice-core data. We
also conducted similar tests with ~1 ml$_{STP}$ sample size using a small test tube, in which whole gas was transferred to a GEPW
tube without splitting. The changes are not significantly different from those of the larger sample sizes (-0.002 ± 0.002, +0.004
460   ± 0.006 and -0.113 ± 0.048 ‰ for $\delta^{15}N$, $\delta^{18}O$ and $\delta Ar/N_2$, respectively (errors are standard error with n = 9)).

Relatively large decrease and dependence on the sample size are found for $\delta O_2/N_2$ in the above tests (-0.193 ± 0.015, -0.293 ±
0.029 and -0.482 ± 0.048 ‰ for 5, 3 and 1 cm$_3$, respectively). We interpret the result as O_2 consumption by the inner walls of
the extraction line and sample tubes, whose magnitude (number of O_2 molecules consumed) might be only weakly dependent
465   on the sample size. We use an exponential fit to the above data (Fig. 6),

$$\Delta\delta_{extraction, O2/N2} = 0.55362 \exp(-0.31606 \times V) - 0.078802 \text{ (‰)}, \tag{7}$$

where V is the sample size of air in ml$_{STP}$ for correcting the ice core data.

4.2.3 Long-term stability of standard gas and atmosphere, and normalization of sample ratios

For normalization of the ice-core data and monitoring its long-term stability, standard gas in a cylinder (STD-A) and
470   atmosphere (sampled outside the NIPR building) have been regularly measured against the reference can.

The atmospheric sampling and measurement procedures follow Headly (2008) and Orsi (2013). Briefly, the atmosphere is
collected in a 1.5 L glass flask with a metal piston pump (Senior Aerospace, MB-158), aspirated air intake and two water traps.
The flow rates of the sampling and aspiration lines are 4 and 15 L min$_{-1}$, respectively, with a flushing time of > 10 min before
475   sampling. In the laboratory, the flask air is expanded into three volumes in series (~4, ~1.5 and ~2 ml) and allowed for 30 min
to equilibrate, and the air in the middle volume is transferred to a GEPW tube. The STD-A is filled in a test tube, and an aliquot
of it is transferred to a GEPW tube using the split line (see section 4.1.2).

The $\delta_{15}N$, $\delta_{18}O$, $\delta O_2/N_2$, and $\delta Ar/N_2$ of STD-A and atmosphere for 2016 to 2019 are shown in Fig. 5 and Fig. 7, and the values

480   of the STD-A against the atmosphere is summarised in Table 5. Shifts in the ratios are commonly seen when the ion source filament or reference can is renewed (as indicated by vertical lines in the figure). However, there are no discernible trends and seasonal variations during the use of one reference can for all ratios except for $\delta O_2/N_2$. Typical standard deviations of a set of atmospheric measurements (~10 replicates) using two flasks within a few days are 0.003, 0.007, 0.020, and 0.034 ‰ for $\delta_{15}N$, $\delta_{18}O$, $\delta O_2/N_2$, and $\delta Ar/N_2$, respectively, while those of the STD-A measurements are 0.004, 0.008, 0.058, and 0.033 ‰,

485   respectively. Comparison of $\delta_{15}N$, $\delta_{18}O$ and $\delta Ar/N_2$ between STD-A and atmosphere indicate slightly better reproducibilities for the atmospheric measurements, possibly due to fractionations during the filling of STD-A into the test tubes. Therefore, the atmosphere is the best choice for the normalization of those ratios.

General trends towards more positive values are seen for $\delta O_2/N_2$ (Fig. 5d and Fig. 7d), presumably because O_2 in the reference

490   can is gradually consumed by oxidation of organic matter on the inner wall. Moreover, atmospheric $\delta O_2/N_2$ in urban areas may show spikes and seasonal variations (Ishidoya and Murayama, 2014), which are much larger than our measurement precision. Indeed, $\delta O_2/N_2$ of STD-A only shows linear trends (due to the drift in the reference can), but the atmospheric $\delta O_2/N_2$ sometimes deviates from its linear trend by up to ~0.5 ‰ (e.g., in Dec. 2017, Jan. 2018, April 2018, Mar. 2019 and Dec. 2019). Thus, the use of a standard gas in the cylinder (STD-A) for normalization, rather than the atmosphere sampled at the time of calibrations,

495   is the better choice for precise $\delta O_2/N_2$ measurements. We here define our "modern air" for $\delta O_2/N_2$ as the annual average $\delta O_2/N_2$ in 2017 observed over Minamitorishima island (hereafter MTS air) (24°17'N, 153°59'E) observed by National Institute of Advanced Industrial Science and Technology (AIST) in cooperation with Japan Meteorological Agency (JMA) (Ishidoya, 2017), and determined $\delta O_2/N_2$ in STD-A against it (+2.595 ± 0.008 ‰). We note that AIST recently developed a gravimetric $\delta O_2/N_2$ calibration scale for precise and long-term atmospheric monitoring (Aoki et al., 2019).

500

The values of atmosphere or STD-A against the reference can within a few weeks immediately before and after the sample measurements are averaged and used for normalizations. The final corrected and normalized δ value of an ice core sample is:

$$\delta_{\text{normalized}} = \left[\frac{(\delta_{\text{slope corrected}} - \Delta\delta_{\text{extraction}}) \cdot 10^{-3} + 1}{\delta_{\text{ATM}} \cdot 10^{-3} + 1} - 1 \right] \cdot 10^3 \; (‰) , \tag{8}$$

where $\Delta\delta_{\text{extraction}}$ is the correction for air extraction and overnight storage (only for $\delta_{15}N$, $\delta O_2/N_2$ and $\delta Ar/N_2$, see section 4.2.2),

505   and δ_{ATM} is the atmospheric value corrected for PIS and chemical slope.

5. Ice core analyses and comparison with published records

We analysed the Dome Fuji (hereafter DF) ice core, Antarctica, and NEEM ice core, Greenland, and compared the results with other records to evaluate the overall reliabilities of our methods. The reproducibilities of ice-core measurements are also assessed using the pooled standard deviation of duplicates (measurements of two ice samples from the same depth,

Atmospheric
Measurement
Techniques
Discussions

510 Severinghaus et al. (2003)) for some depths. The number of samples and depths are as follows: 49 samples from 40 depths in 112.88 – 157.81 m (bubbly ice, 2.0 – 0.2 kyr BP), and 70 samples from 35 depths in 1245.00 – 1918.59 m (clathrate ice, 79 – 150 kyr BP) from the DF core, and 75 samples from 47 depths in 112.68 – 449.10 m (bubbly ice and above brittle zone, 2.0 – 0.2 kyr BP) from the NEEM core.

515 We employed the following age scales and synchronizations. For the preindustrial late Holocene (~0 to ~1800 year C.E.), the GICC05 chronology was used for the NEEM core as published by Rasmussen et al. (2013), and a WAIS Divide Core gas chronology (WDC05A) (Mitchell et al., 2013; Mitchell et al., 2011) was transferred to the DF core by CH_4 synchronization (the tie points are shown in Fig. 9 and Table 6). For the other ice cores for comparisons (including GISP2, WDC, Law Dome cores), we employed their own published time scales (Table A1).

520

The following data were rejected or not acquired due to experimental errors. The DF sample at 144.75 m lost CH_4, CO_2 and N_2O concentrations and TAC because of a connection failure between the GC and computer. $\delta^{15}N$, $\delta^{18}O$, $\delta O_2/N_2$ and $\delta Ar/N_2$ from the DF core at 1521.06, 1540.56 and 1712.10 m were rejected because of the leaky valve on the GEPW tube. The NEEM sample at 217.15 m showed anomalous CO_2 and N_2O concentrations as compared with another sample at the same depth (+83 525 ppm and +47 ppb, respectively); all GC data including CH_4 were rejected for this sample. The NEEM sample at 229.80 m and 438.83 m showed anomalously low $\delta^{15}N$ and $\delta^{18}O$ (half of the typical values, or lower), possibly due to gas handling error or leak. As all the anomalous NEEM data were acquired within 2 months after establishing the method, there would have been experimental errors that slipped from our attention.

5.1 CH_4, N_2O and CO_2 concentrations

530 The pooled standard deviations of the CH_4, N_2O and CO_2 concentrations are ± 3.2 ppb, ± 1.3 ppb and ± 3.2 ppm for the DF bubbly ice (number of pairs = 8), ± 3.3 ppb, ± 2.2 ppb and ± 3.1 ppm for the DF clathrate ice (n = 29), and ± 2.9 ppb, ± 3.0 ppb and ± 5.5 ppm for the NEEM bubbly ice (n = 25) (Table 7). The pooled standard deviations of CH_4 and N_2O are similar to those reported from most precise measurements by other laboratories (± 2.8 ppb for CH_4 by OSU (Mitchell et al., 2013), and ± 1.5 ppb for N_2O by Seoul National University (Ryu et al., 2018)).

535

Our new CH_4, N_2O and CO_2 data from the DF core agree with the previous data from Tohoku University (Fig. 8) (Kawamura, 2001), indicating consistency of the TU concentration scales for ice core analyses over the past ~ 20 years. We compare our results for the preindustrial late Holocene (~0 to ~1800 C.E.) at ~50-year resolution with other ice core records from other groups on the NOAA concentration scales (Fig. 9). The DF CH_4 data agree well with those from the WAIS Divide core by 540 OSU (Mitchell et al., 2013) and Law Dome cores by CSIRO (Rubino et al., 2019), which are currently the best Antarctic records in terms of precision and resolution (see Fig. A1 in Appendix for comparison with other records). We note that multi-decadal variations are smoothed out in the DF core because of the slow bubble-trapping process. For Greenland, our NEEM

data show good agreement with the GISP2 data from OSU (Mitchell et al., 2013), including multidecadal to centennial-scale variations.

545

We note that unrealistically high CH_4 variabilities were found at two depths in the NEEM core (417.60 – 418.00 m and 361.05 – 361.35 m; gas ages are ~218 C.E. and ~532 C.E., respectively) (Fig. 10). The change of ~20 to 50 ppb between the neighbouring depths (only < 1 year apart in age) is impossible to be an atmospheric origin considering diffusive mixing in firn. The good agreements between the duplicate measurements for these depths exclude the possibility of analytical error. The N_2O

550   concentrations at the same depths are not significantly different from those in the neighbouring depths, suggesting that the CH_4 anomalies are not due to ice-sheet surface melt and associated gas dissolution, which should elevate both CH_4 and N_2O. In any case, we exclude these anomalously high concentrations from the calculation of pooled standard deviation and comparison with other ice core records. The CH_4 concentration of 723.7 ppb at 961 C.E. (the mean of four discrete measurements), in the middle of an increase over a century, is also higher than the GISP2 data by ~30 ppb. The four discrete values agree within 12

555   ppb (717.6, 724.9, 729.5 and 722.9 ppb), indicating again that the large deviation from the GISP2 data is not due to analytical error. The reason for this discrepancy is not clear, but it could be due to uncertainty in age synchronization between the cores, a reversal of the NEEM gas age by firn layering (the possibility that the bubbles were closed-off in the last stage of firn-ice transition, Rhodes et al. (2016)) or natural artefacts (e.g., gas dissolution by surface melt, or biological CH_4 production within the ice sheet).

560

N_2O concentrations from both polar regions should agree with each other within the uncertainty of ice core analyses. Our data from the NEEM core agree with those from the Law Dome core by CSIRO within ~5 ppb without systematic bias (Rubino et al., 2019) (see Fig. A1 in Appendix for comparison with other records). The DF data also agree with the NEEM data within ~5 ppb. The sample at 1076 C.E. (129.16 m) of the DF core shows very high concentration (~20 ppb higher than the neighbouring depths), which is unlikely to be due to experimental errors because the CH_4 and CO_2 concentrations of the same

565   sample are not elevated. Anomalous N_2O concentrations were also found in late Holocene DF samples in previous measurements (Kawamura, 2001), and they are possibly natural artefacts (N_2O production in ice sheet) (Kawamura, 2001; Sowers, 2001).

570   The overall agreements of our CH_4 and N_2O data with the other datasets suggest the reliability of our method and consistency of the TU scales at low concentrations with the NOAA scales. We note that our method does not apply experimental corrections for CH_4 and N_2O concentrations. For reference, the OSU method (wet extraction with refreezing) applies solubility correction of 1 % (~3 – 8 ppb) and blank correction of 2.5 ppb for CH_4 (Mitchell et al., 2011), and the CSIRO method (dry extraction) applies blank corrections of 4.1 ppb and 1.8 ppb for CH_4 and N_2O, respectively (MacFarling Meure et al., 2006). The negligible

575   effect of gas dissolution in our method is explained by the immediate removal of the released air from the ice vessel, maintaining low pressure above the meltwater.

The CO_2 concentration is generally measured with dry extraction methods (e.g., (Ahn et al., 2009; Barnola et al., 1987; Monnin et al., 2001; Nakazawa et al., 1993a), because wet extraction method has a risk of contamination by acid-carbonate reaction and oxidation of organic materials in meltwater. While CO_2 production in the meltwater indeed occurs, its magnitude is up to 20 ppm, and the glacial-interglacial CO_2 variations are well captured in the DF record for the last 340 kyr BP (Kawamura et al., 2003). Our new wet-extraction CO_2 values of the DF core for the last 2000 years agree with the Law Dome (MacFarling Meure et al., 2006), EDML (Siegenthaler et al., 2005) and WAIS Divide (Ahn et al., 2012) ice cores mostly within 0 to +10 ppm, with several ~20-ppm deviations. The NEEM wet-extraction CO_2 data are higher than those of DF and other ice cores by ~10 – 30 ppm (maximum ~60 ppm), which is much larger than the pooled standard deviation (5.3 ppm for the NEEM dataset). The primary reason for the high CO_2 values in the NEEM ice core is high impurity contents in the core, which cause in-situ CO_2 production in the ice sheet (Anklin et al., 1995).

5.2 Elemental and isotopic compositions of N_2, O_2 and Ar

5.2.1 Gas-loss fractionation and surface removal

Previous studies have indicated that gases can slightly be lost from ice cores during storage, causing size- and mass-dependent fractionations in $\delta O_2/N_2$, $\delta^{18}O$ and $\delta Ar/N_2$ (Bender et al., 1995; Bereiter et al., 2009; Huber et al., 2006a; Ikeda-Fukazawa et al., 2005; Kawamura et al., 2007; Severinghaus et al., 2009). To examine whether those ratios as originally recorded in the ice sheet can be obtained from the DF core, which had been stored at -50 °C for ~20 years, we measured samples from the same depths but with different thickness of surface removal (for example, 8 and 5 mm) (Fig. 11). The outer ice were also measured and compared with the values from the inner ice.

First, we compare the data from the outer ice and inner ice to validate the magnitude of gas-loss induced fractionation. For both the bubbly ice and clathrate ice (note that bubble-clathrate transition zone is not investigated), all the measured samples show lower $\delta O_2/N_2$ and $\delta Ar/N_2$ in the outer ice than those in the inner ice (Fig. 12). The outer ice has more depleted $\delta O_2/N_2$ and $\delta Ar/N_2$ than the inner ice, and $\delta O_2/N_2$ is more depleted than $\delta Ar/N_2$, indicating significant size-dependent fractionation in the outer ice. Most samples show higher $\delta^{18}O$ in the outer ice than in the inner ice, while $\delta^{15}N$ from the outer and inner ice agree to each other, suggesting that significant mass-dependent fractionation also occurred for O_2, but not for N_2, in the outer ice.

Next, we examine the $\delta O_2/N_2$ data from the inner ice with different thicknesses of surface removal. Below 1380 m (pure clathrate ice), the $\delta O_2/N_2$ values from the inner ice with the outer removal of 5 mm are mostly lower than those from the adjacent pieces with 8-mm removal (Fig. 13), suggesting that gas loss affects the gas composition to more than 5 mm from the

Atmospheric
Measurement
Techniques
Discussions

Open Access
EGU

surface. On the other hand, no significant differences are observed between $\delta O_2/N_2$ values from ice with the removal of more

610 than 8 mm (Fig. 14). The $\delta Ar/N_2$, $\delta^{15}N$ and $\delta^{18}O$ data from the inner ice with surface removal of 5 mm and 8 mm are not different from each other, suggesting insignificant mass-dependent gas-loss fractionation in ice > 5 mm away from the surface. From these results, we conclude that the removal of more than 8 mm is sufficient to obtain the gas composition as originally trapped in the DF1 core.

5.2.2 Reproducibility and comparison with previous data

615 The pooled standard deviations for the DF clathrate hydrate ice with removal thickness of >8 mm are 0.006, 0.010, 0.089 and 0.115 ‰ for $\delta^{15}N$, $\delta^{18}O$, $\delta O_2/N_2$ and $\delta Ar/N_2$, respectively (Table 7). The reproducibility of $\delta O_2/N_2$ is one order of magnitude better than those previously reported (Bender, 2002; Extier et al., 2018). The reproducibility for $\delta^{15}N$ and $\delta^{18}O$ are comparable to but slightly worse than the most precise measurements by SIO (Seltzer et al., 2017; Severinghaus et al., 2009).

620 We compare our new DF data with previous data from Tohoku University (Fig. 15) (Kawamura, 2001; Kawamura et al., 2007). The previous $\delta O_2/N_2$ data were significantly depleted due to gas loss during the sample storage at -25 °C (Fig. 15c, grey marks), thus they were corrected for effect by assuming a linear relationship between the storage duration and $\delta O_2/N_2$ (Fig. 15c, red marks). Our new $\delta O_2/N_2$ data agree with the gas-loss corrected old data, suggesting that $\delta O_2/N_2$ as originally trapped in the DF core can be measured from the 20-year old samples. The new $\delta^{15}N$ and $\delta^{18}O$ data generally agree with those of Kawamura

625 (2001) and Kawamura et al. (2007) within the uncertainty of the old data, although the large uncertainties of the old datasets do not permit precise comparisons.

The duplicate measurements of bubbly ice of the NEEM core (by removing more than 3 mm from the surface) produced pooled standard deviations for $\delta^{15}N$ and $\delta^{18}O$ (0.006 and 0.008 ‰) similar to those for the DF clathrate ice (Table 7). This suggests

630 that the removal of 3 mm is sufficient for the bubbly ice at least for the isotopic ratios, possibly due to generally low pressure of bubbly ice (because it is shallower) compared with clathrate ice. On the other hand, pooled standard deviations for $\delta O_2/N_2$ and $\delta Ar/N_2$ of the bubble ice are much larger than those for the DF clathrate ice (0.236 and 0.120 ‰ for the DF core, and 0.775 and 0.450 ‰ for the NEEM core, respectively), possibly related with the natural variability of pressure and composition of individual air bubbles with different trapping histories (Ikeda-Fukazawa et al., 2001; Kobashi et al., 2015). The larger pooled

635 standard deviations for the NEEM core than those of the DF core possibly reflect natural difference within the ice sheets, or artefacts (gas loss) during drilling, handling and storage at the NEEM site associated with the warmer environment than the Dome Fuji drilling site. We also note that, due to the small number of duplicates for the bubbly ice, it is difficult at this stage to assess whether there are small systematic lowering of $\delta O_2/N_2$ and $\delta Ar/N_2$ with the 3-mm removal.

Atmospheric
Measurement
Techniques
Discussions

Open Access

EGU

5.3 Total air content

The pooled standard deviations for TAC are 0.66 and 0.67 ml_{STP} kg_{-1} for both DF bubbly ice and clathrate ice. The data from the clathrate ice agree with those from previous measurements using ~300 g of ice (Kawamura, 2001), while the data from the bubbly ice appear to be lower than the previous data, especially for the shallowest depths (Fig. 15). These results may be explained by the fact that TAC of bubbly ice is biased towards lower values due to the so-called "cut-bubble effect" (Martinerie et al., 1990), in which bubbles intersecting the sample surfaces are cut and lose air. The cut-bubble effect is larger for samples with a smaller surface-to-volume ratio and samples from shallower depths.

6. Conclusions

We presented a new analytical technic for high-precision, simultaneous measurements of CH_4, N_2O and CO_2 concentrations, isotopic and elemental ratios of N_2, O_2 and Ar, and total air content, from a single ice core sample with relatively small size (50 – 70 g) by a wet extraction. The ice sample is melted under vacuum in 3 min, and the released air is continuously transferred and cryogenically trapped into a sample tube, with the total duration for extraction of about 10 minutes. The rapid and continuous transfer minimizes contaminations due to degassing from the inner walls of the apparatus, as well as dissolution of the sample air into the meltwater. The extracted air is homogenized in the sample tube for one night, and split into two aliquots for mass spectrometric measurement (~20 % of the sample) and gas chromatographic measurement (~80 % of the sample).

The system performance was evaluated by measuring the standard gas after treating it as the ice-core air extraction, by passing it through the extraction and split lines with gas-free water in the extraction vessel. We do not observe significant changes in the mean CH_4, N_2O and CO_2 concentrations, possibly because of the long evacuation, rapid and continuous gas transfer at low pressure over meltwater, and passivation treatments of the extraction lines and sample tubes. Thus, we do not apply corrections (e.g., so-called blank correction and solubility correction) for the greenhouse gas concentrations. For the mass spectrometry, we do not observe significant changes in $\delta_{18}O$, while we observe changes in $\delta_{15}N$, $\delta O_2/N_2$, $\delta Ar/N_2$. Moreover, the change in $\delta O_2/N_2$ is dependent on the sample size. Thus, we apply constant corrections for $\delta_{15}N$ and $\delta Ar/N_2$, and sample-size-dependent correction for $\delta O_2/N_2$.

Standard deviations of duplicate measurements for DF clathrate ice are 3.2 ppb, 2.2 ppb, and 3.1 ppm for CH_4, N_2O and CO_2 concentrations, respectively, and 0.006, 0.010, 0.09 and 0.12 ‰ for $\delta_{15}N$, $\delta_{18}O$, $\delta O_2/N_2$ and $\delta Ar/N_2$, respectively. The CH_4 and N_2O data from the DF and NEEM ice cores for the last 2,000 years agree well with those from the GISP2, WAIS Divide and Law Dome cores. We also demonstrate significant gas-loss induced depletion of $\delta O_2/N_2$ in the ice near the sample surface of the DF clathrate ice, which has been stored at -50 °C over ~20 years. The original $\delta O_2/N_2$, $\delta Ar/N_2$, $\delta_{15}N$ and $\delta_{18}O$ in the ice sheet may still be obtained by removing the sample surface by > 8 mm.

Atmospheric
Measurement
Techniques
Discussions

Our new method will have many paleoclimatic applications, such as detecting subtle variations in greenhouse gas cycles (in particular CH_4 inter-polar difference and N_2O variations), hydrological cycles ($\delta^{18}O$ of O_2), insolation signals for dating ($\delta O_2/N_2$ and $\delta Ar/N_2$), and local climatic and glaciological conditions ($\delta^{15}N$ and TAC) from deep ice cores with high temporal resolution.

Data availability

Gas data of the Dome Fuji and NEEM ice cores are available at the NIPR ADS data repository (https://ads.nipr.ac.jp/dataset/A20200501-001; for inquiry: oyabu.ikumi@nipr.ac.jp).

Author contribution

K. Kawamura designed the wet extraction apparatus and mass spectrometer configuration, and developed the overall concept of the splitting and multiple-species analyses. K. Kawamura, SS and AK designed the GC configurations. JPS and RB developed the calibration protocols for atmospheric normalization of mass spectrometer measurements except for $\delta O_2/N_2$, and customized ISODAT scripts. RD developed GC controlling software with discussion with K. Kawamura. SI provided the $\delta O_2/N_2$ standard scale. DDJ provided the NEEM ice core samples. KGA provided funding for the mass spectrometer, and the NEEM samples as the national representative. SA and TN provided the greenhouse gas concentration scales and funding for the wet extraction apparatus and cryostat. IO and K. Kitamura made the measurements. IO, K. Kitamura and K. Kawamura established the detailed procedures of ice core measurements and calibrations. CS contributed to the early stages of development. IO and K. Kawamura wrote the manuscript, and all authors contributed to the discussion.

Competing interests

The authors declare that they have no conflict of interest.

References

Ahn, J., Brook, E. J., and Howell, K.: A high-precision method for measurement of paleoatmospheric CO_2 in small polar ice samples, J. Glaciol., 55, 499-506, https://doi.org/10.3189/002214309788816731, 2009.

Ahn, J., Brook, E. J., Mitchell, L., Rosen, J., McConnell, J. R., Taylor, K., Etheridge, D., and Rubino, M.: Atmospheric CO_2

710 over the last 1000 years: A high-resolution record from the West Antarctic Ice Sheet (WAIS) Divide ice core, Global Biogeochem. Cycles, 26, https://doi.org/10.1029/2011GB004247, 2012.

Anklin, M., Barnola, J. M., Schwander, J., Stauffer, B., and Raynaud, D.: Processes Affecting the CO_2 Concentrations Measured in Greenland Ice, Tellus B, 47, 461-470, https://doi.org/10.1034/j.1600-0889.47.issue4.6.x, 1995.

Aoki, N., Ishidoya, S., Matsumoto, N., Watanabe, T., Shimosaka, T., and Murayama, S.: Preparation of primary standard

715 mixtures for atmospheric oxygen measurements with less than 1 µmol mol^{-1} uncertainty for oxygen molar fractions, Atmos. Meas. Tech., 12, 2631-2646, https://doi.org/10.5194/amt-12-2631-2019, 2019.

Aoki, S., Nakazawa, T., Murayama, S., and Kawaguchi, S.: Measurements of atmospheric methane at the Japanese Antarctic Station, Syowa, Tellus, 44, 273-281, https://doi.org/10.3402/tellusb.v44i4.15455, 1992.

Barnola, J. M., Raynaud, D., Korotkevich, Y. S., and Lorius, C.: Vostok Ice Core Provides 160,000-Year Record of

720 Atmospheric CO_2, Nature, 329, 408-414, https://doi.org/10.1038/329408a0, 1987.

Bazin, L., Landais, A., Lemieux-Dudon, B., Toyé Mahamadou Kele, H., Veres, D., Parrenin, F., Martinerie, P., Ritz, C., Capron, E. F. N., Lipenkov, V., Loutre, M. F., Raynaud, D., Vinther, B., Svensson, A., Rasmussen, S. O., Severi, M., Blunier, T., Leuenberger, M., Fischer, H., Masson-Delmotte, V., Chappellaz, J., and Wolff, E.: An optimized multi-proxy, multi-site Antarctic ice and gas orbital chronology (AICC2012): 120-800 ka, Clim. Past, 9, 1715-1731,

725 https://doi.org/10.5194/cp-9-1715-2013, 2013.

Beck, J., Bock, M., Schmitt, J., Seth, B., Blunier, T., and Fischer, H.: Bipolar carbon and hydrogen isotope constraints on the Holocene methane budget, Biogeosciences, 15, 7155-7175, https://doi.org/10.5194/bg-15-7155-2018, 2018.

Bender, M., Sowers, T., and Lipenkov, V.: On the concentrations of O_2, N_2, and Ar in trapped gases from ice cores, J. Geophys. Res., https://doi.org/10.1029/94JD02212, 1995.

730 Bender, M. L.: Orbital tuning chronology for the Vostok climate record supported by trapped gas composition, Earth Planet. Sci. Lett, 204, 275-289, https://doi.org/10.1016/S0012-821X(02)00980-9, 2002.

Bereiter, B., Kawamura, K., and Severinghaus, J. P.: New methods for measuring atmospheric heavy noble gas isotope and elemental ratios in ice core samples, Rapid Commun. Mass Spectrom., 32, 801-814, doi/10.1002/rcm.8099, 2018.

Bereiter, B., Schwander, J., Luthi, D., and Stocker, T. F.: Change in CO_2 concentration and O_2/N_2 ratio in ice cores due to

735 molecular diffusion, Geophys. Res. Lett., 36, L05703-05705, https://doi.org/10.1029/2008GL036737, 2009.

Atmospheric
Measurement
Techniques
Discussions
Open Access

Blunier, T. and Brook, E. J.: Timing of millennial-scale climate change in Antarctica and Greenland during the last glacial period, Science, 291, 109-112, https://doi.org/10.1126/science.291.5501.109, 2001.

Blunier, T., Chappellaz, J., Schwander, J., Stauffer, B., and Raynaud, D.: Variations in atmospheric methane concentration during the Holocene epoch, Nature, 374, 46-49, https://doi.org/10.1038/374046a0, 1995.

740   Bock, M., Schmitt, J., Beck, J., Seth, B., Chappellaz, J., and Fischer, H.: Glacial/interglacial wetland, biomass burning, and geologic methane emissions constrained by dual stable isotopic CH_4 ice core records, Proc. Natl. Acad. Sci. USA., 114, E5778-E5786, https://doi.org/10.1073/pnas.1613883114, 2017.

Author: Methane measurements from the GISP2 and Siple Dome ice cores, U.S. Antarctic Program (USAP) Data Center, https://doi.org/10.7265/N58P5XFZ, 2009.

745   Brook, E. J., Sowers, T., and Orchardo, J.: Rapid variations in atmospheric methane concentration during the past 110,000 years, Science, 273, 1087-1091, https://doi.org/10.1126/science.273.5278.1087, 1996.

Brook, E. J., White, J. W. C., Schilla, A. S. M., Bender, M. L., Barnett, B., Severinghaus, J. P., Taylor, K. C., Alley, R. B., and Steig, E. J.: Timing of millennial-scale climate change at Siple Dome, West Antarctica, during the last glacial period, Quat. Sci. Rev., 24, 1333-1343, https://doi.org/10.1016/j.quascirev.2005.02.002, 2005.

750   Chappellaz, J., Blunier, T., Kints, S., Dällenbach, A., Barnola, J.-M., Schwander, J., Raynaud, D., and Stauffer, B.: Changes in the atmospheric CH_4 gradient between Greenland and Antarctica during the Holocene, J. Geophys. Res., 102, 15987-15997, https://doi.org/10.1029/97JD01017, 1997.

Chappellaz, J. A., Fung, I. Y., and Thompson, A. M.: The atmospheric CH_4 increase since the Last Glacial Maximum, Tellus, 45, 228-241, https://doi.org/10.3402/tellusb.v45i3.15726, 1993.

755   Dlugokencky, E. J.: Conversion of NOAA atmospheric dry air CH_4 mole fractions to a gravimetrically prepared standard scale, J. Geophys. Res., 110, https://doi.org/10.1029/2005JD006035, 2005.

Extier, T., Landais, A., Bréant, C., Prié, F., Bazin, L., Dreyfus, G., Roche, D. M., and Leuenberger, M.: On the use of $\delta_{18}O_{atm}$ for ice core dating, Quat. Sci. Rev., 185, 244-257, https://doi.org/10.1016/j.quascirev.2018.02.008, 2018.

Flückiger, J., Dällenbach, A., Blunier, T., Stauffer, B., Stocker, T. F., Raynaud, D., and Barnola, J. M.: Variations in
760   atmospheric N_2O concentration during abrupt climatic changes, Science, 285, 227-230, https://doi.org/10.1126/science.285.5425.227, 1999.

Flückiger, J., Moon, J., Stauffer, B., Schwander, J., and Stocker, T. F.: High-resolution Holocene N_2O ice core record and its relationship with CH_4 and CO_2, Global Biogeochem. Cycles, 16, 1010, https://doi.org/10.1029/2001GB001417, 2002.

Headly, M.: Krypton and xenon in air trapped in polar ice cores: paleo-atmospheric measurements for estimating past mean
765   ocean temperature and summer snowmelt frequency, Ph. D thesis, UC San Diego, USA, ProQuest ID: umi-ucsd-2223. Merritt ID: ark:/20775/bb7065849g, Retrieved from https://escholarship.org/uc/item/7065845jv7065849j7065846kw, 2008.

Huber, C., Beyerle, U., Leuenberger, M., Schwander, J., Kipfer, R., Spahni, R., Severinghaus, J. P., and Weiler, K.: Evidence for molecular size dependent gas fractionation in firn air derived from noble gases, oxygen, and nitrogen measurements, Earth Planet. Sci. Lett, 243, 61-73, https://doi.org/10.1016/j.epsl.2005.12.036, 2006a.

770   Huber, C., Leuenberger, M., Spahni, R., Flückiger, J., Schwander, J., Stocker, T. F., Johnsen, S., Landais, A., and Jouzel, J.: Isotope calibrated Greenland temperature record over Marine Isotope Stage 3 and its relation to CH_4, Earth Planet. Sci. Lett, 243, 504-519, https://doi.org/10.1016/j.epsl.2006.01.002, 2006b.

Ikeda-Fukazawa, T., Fukumizu, K., Kawamura, K., Aoki, S., Nakazawa, T., and Hondoh, T.: Effects of molecular diffusion on trapped gas composition in polar ice cores, Earth Planet. Sci. Lett, 229, 183-192,
775   https://doi.org/doi:10.1016/j.epsl.2004.11.011, 2005.

Ikeda-Fukazawa, T., Hondoh, T., Fukumura, T., Fukazawa, H., and Mae, S.: Variation in N_2/O_2 ratio of occluded air in Dome Fuji Antarctic ice, J. Geophys. Res., 106, 17799-17810, https://doi.org/10.1029/2000JD000104, 2001.

Ishidoya, S. and Murayama, S.: Development of a new high precision continuous measuring system for atmospheric O_2/N_2 and Ar/N_2 and its application to the observation in Tsukuba, Japan, Tellus B, 66, 22574, https://doi.org/10.3402/tellusb.v66.22574, 2014.

Ishidoya, S., Tsuboi, K., Murayama, S., Matsueda, H., Aoki, N., Shimosaka, T., Kondo, H., and Saito, K.: Development of a continuous measurement system for atmospheric O_2/N_2 ratio using a Paramagnetic analyzer and its application in Minamitorishima Island, Japan, SOLA, 13, 230-234, https://doi.org/10.2151/sola.2017-042, 2017.

Ishijima, K., Nakazawa, T., Sugawara, S., Aoki, S., and Saeki, T.: Concentration variations of tropospheric nitrous oxide over Japan, Geophys. Res. Lett., 28, 171-174, https://doi.org/10.1029/2000GL011465, 2001.

Kawamura, K.: Variations of atmospheric components over the past 340000 years from Dome Fuji deep ice core, Antarctica, Ph. D thesis, Tohoku University, Japan, http://hdl.handle.net/10097/38833, 2001.

Kawamura, K., Nakazawa, T., Aoki, S., Sugawara, S., Fujii, Y., and Watanabe, O.: Atmospheric CO_2 variations over the last three glacial-interglacial climatic cycles deduced from the Dome Fuji deep ice core, Antarctica using a wet extraction technique, Tellus B, 55, 126-137, https://doi.org/10.1034/j.1600-0889.2003.00050.x, 2003.

Kawamura, K., Parrenin, F., Lisiecki, L., Uemura, R., Vimeux, F., Severinghaus, J. P., Hutterli, M. A., Nakazawa, T., Aoki, S., Jouzel, J., Raymo, M. E., Matsumoto, K., Nakata, H., Motoyama, H., Fujita, S., Goto-Azuma, K., Fujii, Y., and Watanabe, O.: Northern Hemisphere forcing of climatic cycles in Antarctica over the past 360,000years, Nature, 448, 912-916, https://doi.org/10.1038/nature06015, 2007.

Kobashi, T., Ikeda-Fukazawa, T., Suwa, M., Schwander, J., Kameda, T., Lundin, J., Hori, A., Motoyama, H., Döring, M., and Leuenberger, M.: Post-bubble close-off fractionation of gases in polar firn and ice cores: effects of accumulation rate on permeation through overloading pressure, Atmos. Chem. Phys., 15, 13895-13914, https://doi.org/10.5194/acp-15-13895-2015, 2015.

Kobashi, T., Kawamura, K., Severinghaus, J. P., Barnola, J.-M., Nakaegawa, T., Vinther, B. M., Johnsen, S. J., and Box, J. E.: High variability of Greenland surface temperature over the past 4000 years estimated from trapped air in an ice core, Geophys. Res. Lett., 38, https://doi.org/10.1029/2011GL049444, 2011.

Kobashi, T., Severinghaus, J. P., and Barnola, J.-M.: 4±1.5 °C abrupt warming 11,270 yr ago identified from trapped air in Greenland ice, Earth Planet. Sci. Lett, 268, 397-407, https://doi.org/10.1016/j.epsl.2008.01.032, 2008.

Landais, A., Dreyfus, G., Capron, E., Masson-Delmotte, V., Sanchez-Goni, M. F., Desprat, S., Hoffmann, G., Jouzel, J., Leuenberger, M., and Johnsen, S.: What drives the millennial and orbital variations of $\delta_{18}O_{atm}$?, Quat. Sci. Rev., 29, 235-246, https://doi.org/10.1016/j.quascirev.2009.07.005, 2010.

Lipenkov, V. Y., Raynaud, D., and Loutre, M. F.: On the potential of coupling air content and O_2/N_2 from trapped air for establishing an ice core chronology tuned on local insolation, Quat. Sci. Rev., 30, 3280-3289, https://doi.org/10.1016/j.quascirev.2011.07.013, 2011.

MacFarling Meure, C., Etheridge, D., Trudinger, C., Steele, P., Langenfelds, R., van Ommen, T., Smith, A., and Elkins, J.: Law Dome CO_2, CH_4 and N_2O ice core records extended to 2000 years BP, Geophys. Res. Lett., 33, L14810, https://doi.org/10.1029/2006GL026152, 2006.

Machida, T., Nakazawa, T., Fujii, Y., Aoki, S., and Watanabe, O.: Increase in the atmospheric nitrous oxide concentration during the last 250 years, Geophys. Res. Lett., 22, 2921-2924, https://doi.org/10.1029/95GL02822, 1995.

Martinerie, P., Lipenkov, V. Y., and Raynaud, D.: Air content paleo record in the Vostok ice core (Antarctica): A mixed record of climatic and glaciological parameters, J. Geophys. Res., 99, 10565-10576, https://doi.org/10.1029/93JD03223, 1994.

Martinerie, P., Lipenkov, V. Y., and Raynaud, D.: Correction of air-content measurements in polar ice for the effect of cut bubbles at the surface of the sample, J. Glaciol., 36, 299-303, https://doi.org/10.3189/002214390793701282, 1990.

Atmospheric
Measurement
Techniques
Discussions

Martinerie, P., Raynaud, D., Etheridge, D. M., Barnola, J. M., and Mazaudier, D.: Physical and climatic parameters which influence the air content in polar ice, Earth Planet. Sci. Lett, 112, 1-13, https://doi.org/10.1016/0012-821X(92)90002-D, 1992.

Mitchell, L., Brook, E., Lee, J. E., Buizert, C., and Sowers, T.: Constraints on the late Holocene anthropogenic contribution to the atmospheric methane budget, Science, 342, 964-966, https://doi.org/10.1126/science.1238920, 2013.

Mitchell, L. E., Brook, E. J., Sowers, T., McConnell, J. R., and Taylor, K.: Multidecadal variability of atmospheric methane, 1000-1800 C.E, Journal of Geophysical Research: Biogeosciences, 116, G02007, https://doi.org/10.1029/2010JG001441, 2011.

Monnin, E., Indermühle, A., Dällenbach, A., Flückiger, J., Stauffer, B., Stocker, T. F., Raynaud, D., and Barnola, J.-M.: Atmospheric CO_2 Concentrations over the Last Glacial Termination, Science, 291, 112-114, https://doi.org/10.1126/science.291.5501.112, 2001.

Nakazawa, T., Machida, T., Esumi, K., Tanaka, M., Fujii, Y., Aoki, S., and Watanabe, O.: Measurements of CO_2 and CH_4 concentrations a polar ice core, J. Glaciol., 39, 209-215, https://doi.org/10.3189/S0022143000015860, 1993a.

Nakazawa, T., Machida, T., Tanaka, M., Fujii, Y., Aoki, S., and Watanabe, O.: Differences of the atmospheric CH_4 concentration between the Arctic and Antarctic regions in pre-industrial/pre-agricultural era, Geophys. Res. Lett., 20, 943-946, https://doi.org/10.1029/93GL00776, 1993b.

NEEM community members: Eemian interglacial reconstructed from a Greenland folded ice core, Nature, 493, 489-494, https://doi.org/10.1038/nature11789, 2013.

Orsi, A. J.: Temperature reconstruction at the West Antarctic Ice Sheet Divide, for the last millennium, from the combination of borehole temperature and inert gas isotope measurements, Ph. D thesis, UC San Diego, USA, ProQuest ID: Orsi_ucsd_0033D_13075, Merritt ID: ark:/20775/bb4779580x, Retrieved from https://escholarship.org/uc/item/4779502g4779583c4779585fq, 2013.

Orsi, A. J., Cornuelle, B. D., and Severinghaus, J. P.: Magnitude and temporal evolution of Dansgaard–Oeschger event 8 abrupt temperature change inferred from nitrogen and argon isotopes in GISP2 ice using a new least-squares inversion, Earth Planet. Sci. Lett, 395, 81-90, https://doi.org/10.1016/j.epsl.2014.03.030, 2014.

Parrenin, F., Cavitte, M. G. P., Blankenship, D. D., Chappellaz, J., Fischer, H., Gagliardini, O., Masson-Delmotte, V., Passalacqua, O., Ritz, C., Roberts, J., Siegert, M. J., and Young, D. A.: Is there 1.5-million-year-old ice near Dome C, Antarctica?, The Cryosphere, 11, 2427-2437, https://doi.org/10.5194/tc-11-2427-2017, 2017.

Prokopiou, M., Sapart, C. J., Rosen, J., Sperlich, P., Blunier, T., Brook, E., van de Wal, R. S. W., and Röckmann, T.: Changes in the isotopic signature of atmospheric nitrous oxide and its global average source during the last three millennia, J. Geophys. Res., 123, 10,757-710,773, https://doi.org/10.1029/2018JD029008, 2018.

Rasmussen, S. O., Abbott, P. M., Blunier, T., Bourne, A. J., Brook, E., Buchardt, S. L., Buizert, C., Chappellaz, J., Clausen, H. B., Cook, E., Dahl-Jensen, D., Davies, S. M., Guillevic, M., Kipfstuhl, S., Laepple, T., Seierstad, I. K., Severinghaus, J. P., Steffensen, J. P., Stowasser, C., Svensson, A., Vallelonga, P., Vinther, B. M., Wilhelms, F., and Winstrup, M.: A first chronology for the North Greenland Eemian Ice Drilling (NEEM) ice core, Clim. Past, 9, 2713-2730, https://doi.org/10.5194/cp-9-2713-2013, 2013.

Rasmussen, S. O., Bigler, M., Blockley, S. P., Blunier, T., Buchardt, S. L., Clausen, H. B., Cvijanovic, I., Dahl-Jensen, D., Johnsen, S. J., Fischer, H., Gkinis, V., Guillevic, M., Hoek, W. Z., Lowe, J. J., Pedro, J. B., Popp, T., Seierstad, I. K., Steffensen, J. P., Svensson, A. M., Vallelonga, P., Vinther, B. M., Walker, M. J. C., Wheatley, J. J., and Winstrup, M.: A stratigraphic framework for abrupt climatic changes during the Last Glacial period based on three synchronized Greenland ice-core records: refining and extending the INTIMATE event stratigraphy, Quat. Sci. Rev., 106, 14-28, https://doi.org/10.1016/j.quascirev.2014.09.007, 2014.

Raynaud, D., Lipenkov, V., Lemieux-Dudon, B., Duval, P., Loutre, M.-F., and Lhomme, N.: The local insolation signature of air content in Antarctic ice. A new step toward an absolute dating of ice records, Earth Planet. Sci. Lett, 261, 337-349, https://doi.org/10.1016/j.epsl.2007.06.025, 2007.

865 Rhodes, R. H., Faïn, X., Brook, E. J., McConnell, J. R., Maselli, O. J., Sigl, M., Edwards, J., Buizert, C., Blunier, T., Chappellaz, J., and Freitag, J.: Local artifacts in ice core methane records caused by layered bubble trapping and in situ production: a multi-site investigation, Clim. Past, 12, 1061-1077, https://doi.org/10.5194/cp-12-1061-2016, 2016.

Rubino, M., Etheridge, D. M., and System, D. P. T. E.: Revised records of atmospheric trace gases CO_2, CH_4, N_2O, and $\delta_{13}C$-CO_2 over the last 2000 years from Law Dome, Antarctica, Earth Syst. Sci. Data, 11, 473-492, https://doi.org/10.5194/essd-11-473-2019, 2019.

870 Ryu, Y., Ahn, J., and Yang, J.-W.: High-Precision Measurement of N_2O Concentration in Ice Cores, Environ. Sci. Technol., 52, 731-738, https://doi.org/10.1021/acs.est.7b05250, 2018.

Schilt, A., Baumgartner, M., Blunier, T., Schwander, J., Spahni, R., Fischer, H., and Stocker, T. F.: Glacial-interglacial and millennial-scale variations in the atmospheric nitrous oxide concentration during the last 800,000 years, Quat. Sci. Rev., 29, 182-192, https://doi.org/10.1016/j.quascirev.2009.03.011, 2010.

875 Seierstad, I., Abbott, M. B., Bigler, M., Blunier, T., Bourne, A. J., Brook, E., Buchardt, S. L., Buizert, C., Clausen, H., Cook, E., Dahl-Jensen, D., Davies, S. M., Guillevic, M., Johnsen, S., Pedersen, D. S., Popp, T., Rasmussen, S. O., Severinghaus, J. P., Svensson, A., and Vinther, B.: Consistently dated records from the Greenland GRIP, GISP2 and NGRIP ice cores for the past 104 ka reveal regional millennial-scale $\delta_{18}O$ gradients with possible Heinrich event imprint, Quat. Sci. Rev., 106, 29-46, https://doi.org/10.1016/j.quascirev.2014.10.032, 2014.

880 Seltzer, A. M., Buizert, C., Baggenstos, D., Brook, E. J., Ahn, J., Yang, J.-W., and Severinghaus, J. P.: Does $\delta_{18}O$ of O_2 record meridional shifts in tropical rainfall?, Clim. Past, 13, 1323-1338, https://doi.org/10.5194/cp-13-1323-2017, 2017.

Severinghaus, J. P., Beaudette, R., Headly, M. A., Taylor, K., and Brook, E. J.: Oxygen-18 of O_2 Records the Impact of Abrupt Climate Change on the Terrestrial Biosphere, Science, 324, 1431-1434, https://doi.org/10.1126/science.1169473, 2009.

Severinghaus, J. P. and Brook, E.: Abrupt climate change at the end of the last glacial period inferred from trapped air in polar Ice, Science, 286, 930-934, https://doi.org/10.1126/science.286.5441.930, 1999.

Severinghaus, J. P., Grachev, A., Luz, B., and Caillon, N.: A method for precise measurement of argon 40/36 and krypton/argon ratios in trapped air in polar ice with applications to past firn thickness and abrupt climate change in Greenland and at Siple Dome, Antarctica, Geochim. Cosmochim. Acta, 67, 325-343, https://doi.org/10.1016/S0016-7037(02)00965-1, 2003.

Severinghaus, J. P., Sowers, T., Brook, E., Alley, R. B., and Bender, M.: Timing of abrupt climate change at the end of the
890 Younger Dryas interval from thermally fractionated gases in polar ice, Nature, 391, 141-146, https://doi.org/10.1038/34346, 1998.

Siegenthaler, U., Monnin, E., Kawamura, K., Spahni, R., Schwander, J., Stauffer, B., Stocker, T. F., Barnola, J.-M., and Fischer, H.: Supporting evidence from the EPICA Dronning Maud Land ice core for atmospheric CO_2 changes during the past millennium, Tellus B, 57, 51-57, https://doi.org/10.3402/tellusb.v57i1.16774, 2005.

895 Sowers, T.: N_2O record spanning the penultimate deglaciation from the Vostok ice core, J. Geophys. Res., 106, 31903-31914, https://doi.org/10.1029/2000JD900707, 2001.

Sowers, T., Alley, R. B., and Jubenville, J.: Ice core records of atmospheric N_2O covering the last 106,000 years, Science, 301, https://doi.org/10.1126/science.1085293, 2003.

Tanaka, M., Nakazawa, T., and Aoki, S.: High Quality Measurements of the Concentration of Atmospheric Carbon Dioxide,
900 Journal of the Meteorological Society of Japan. Ser. II, 61, 678-685, https://doi.org/10.2151/jmsj1965.61.4_678, 1983.

Tanaka, M., Nakazawa, T., Shiobara, M., Ohshima, H., Aoki, S., Kawaguchi, S., Yamanouchi, T., Makino, Y., and Murayama, H.: Variations of atmospheric carbon dioxide concentration at Syowa Station (69°00'S, 39°35'E), Antarctica, Tellus B, 39, 72, doi/10.3402/tellusb.v39i1-2.15324, 1987.

Tsuboi, K., Nakazawa, T., Matsueda, H., Machida, T., Aoki, S., Morimoto, S., Goto, D., Shimosaka, T., Kato, K., Aoki, N.,
905   Watanabe, T., Mukai, H., Thojima, Y., Katsumata, K., Murayama, S., Ishidoya, S., Fujitani, T., Koide, H., Takahashi, M.,
Kawasaki, T., Takizawa, A., and Sawa, Y.: InterComparison Experiments for Greenhouse Gases Observation (iceGGO) in
2012–2016, Technical Reports of the Meteorological Research Institute, 79, https://doi.org/10.11483/mritechrepo.79, 2017.

WAIS Divide Project Members: Precise interpolar phasing of abrupt climate change during the last ice age, Nature, 520, 661-
665, https://doi.org/10.1038/nature14401, 2015.

910
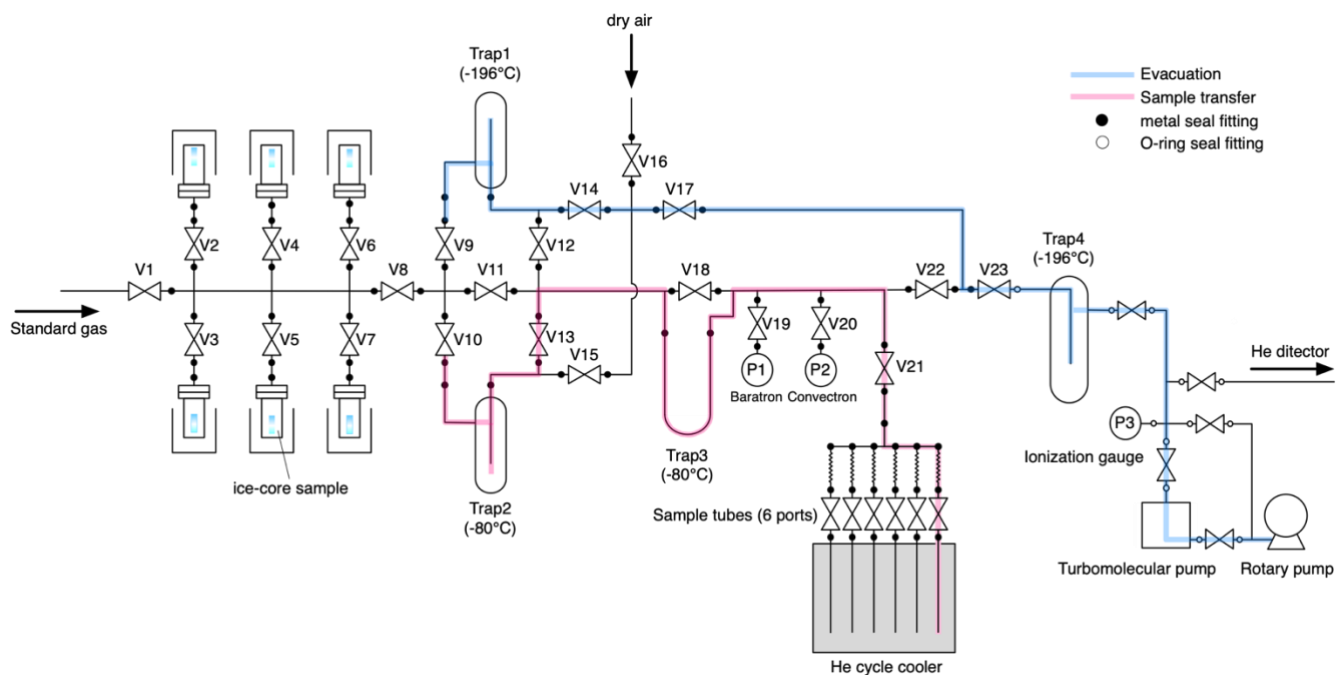
Figures

Figure 1: Schematic diagram of the wet extraction system.

915

920
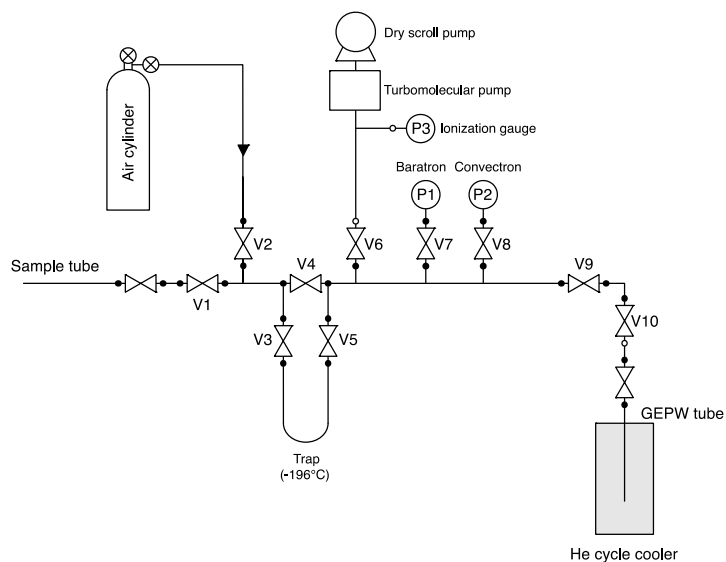
Figure 2: Schematic diagram of the split line.

925

Atmospheric
Measurement
Techniques
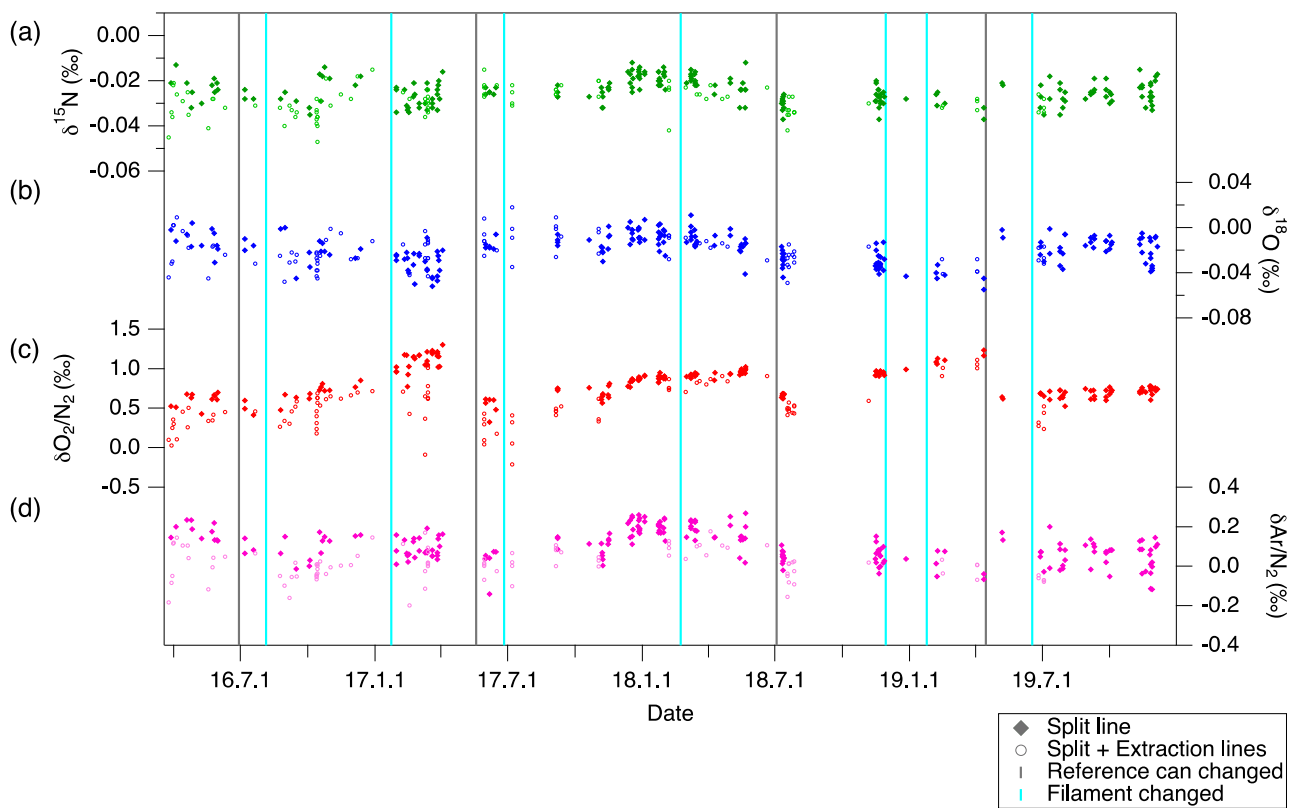Discussions
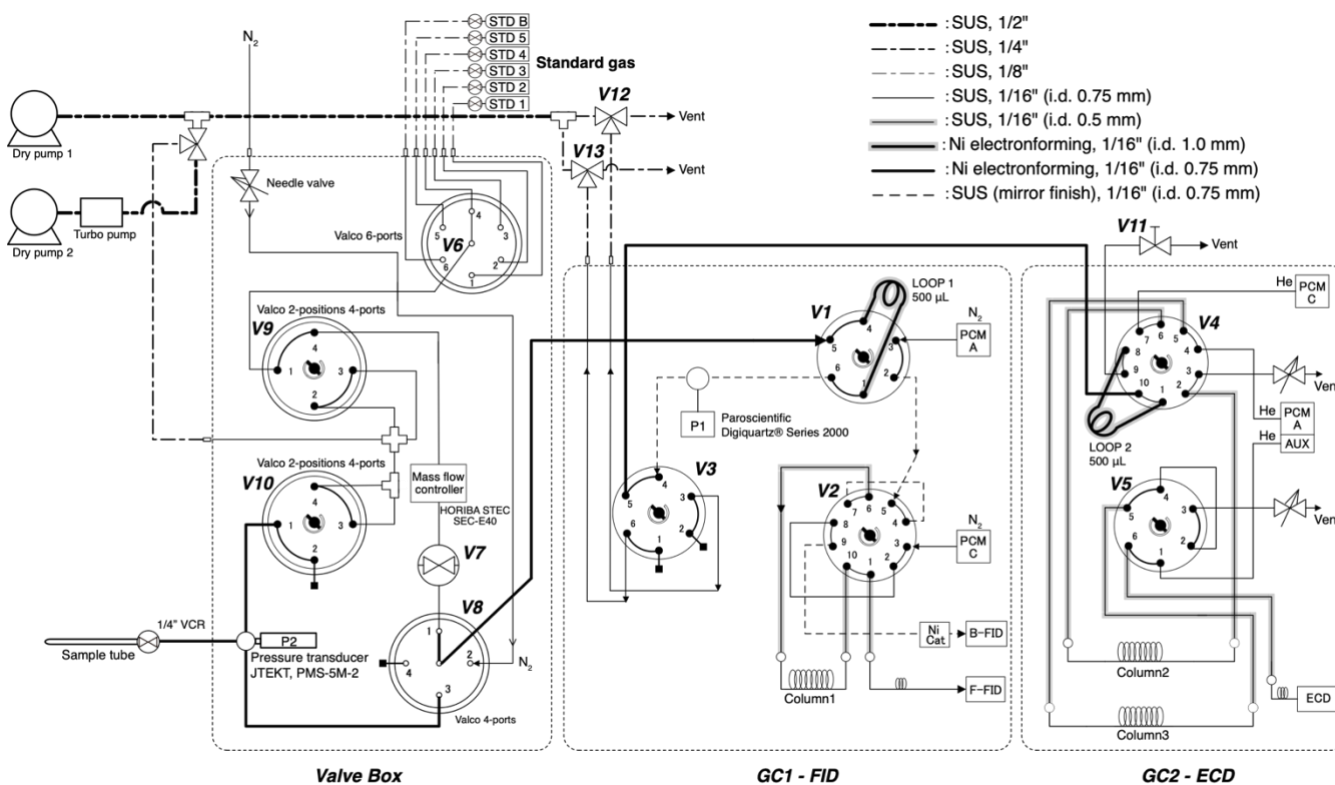
Figure 3: Schematic diagram of gas chromatographs and inlet. All two-position valves are in "OFF" positions.

Atmospheric
Measurement
Techniques
Discussions
Open Access
EGU
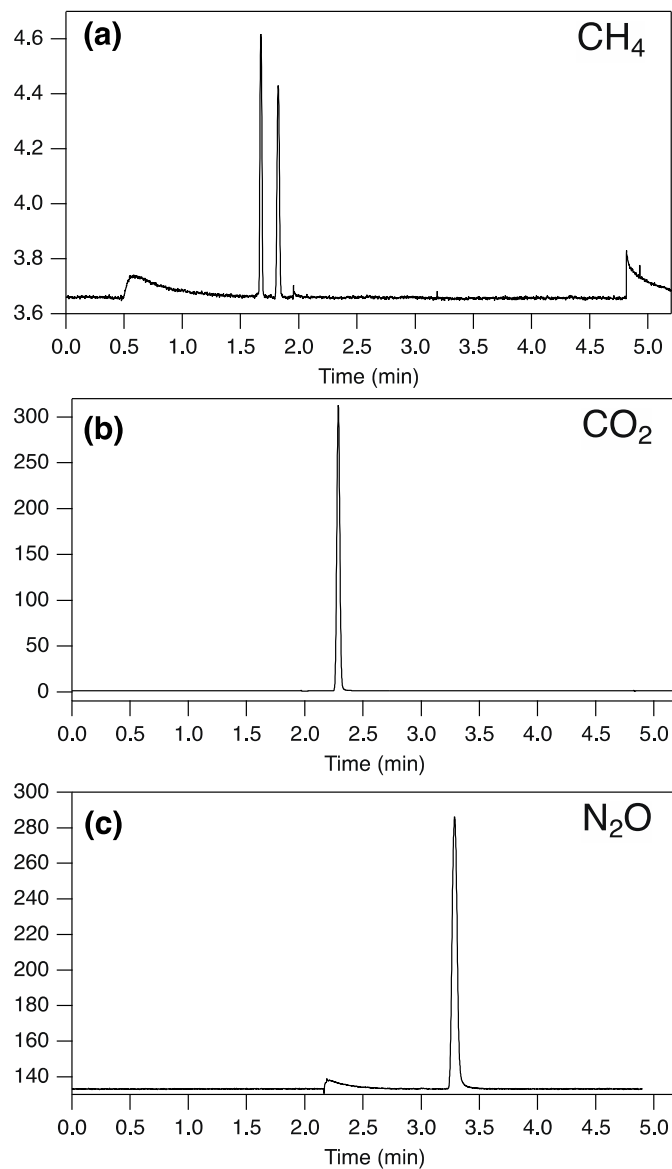
930

Figure 4: Typical chromatogram of (a) Front FID for CH_4 (the largest peak is O_2, and the second-largest peak is CH_4), (b) Back FID for CO_2, and (c) ECD for N_2O.
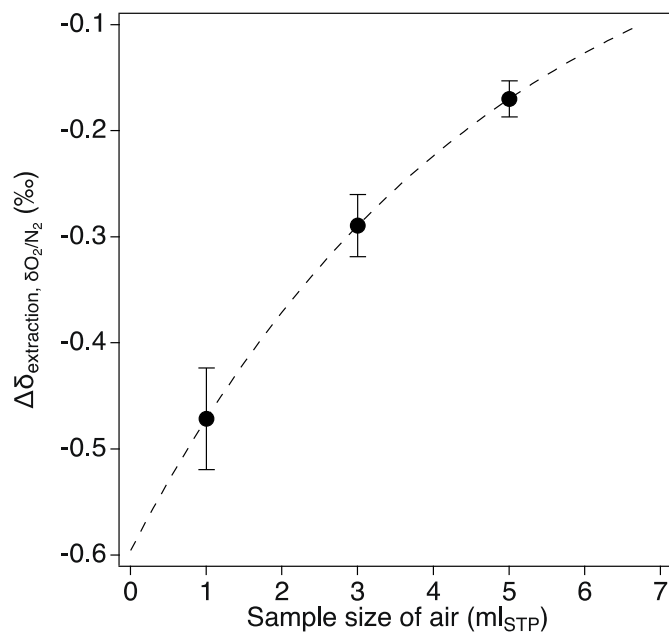
Figure 5: Standard gas (STDA) composition measured against reference gas for (a) $\delta^{15}N$, (b) $\delta^{18}O$, (c) $\delta O_2/N_2$, and (d) $\delta Ar/N_2$. Filled markers represent samples transferred only through the split line, and open markers represent samples transferred through both extraction and split lines. Vertical grey lines indicate the timing of replacements of reference can, and vertical light blue lines indicate the timing of filament replacements.
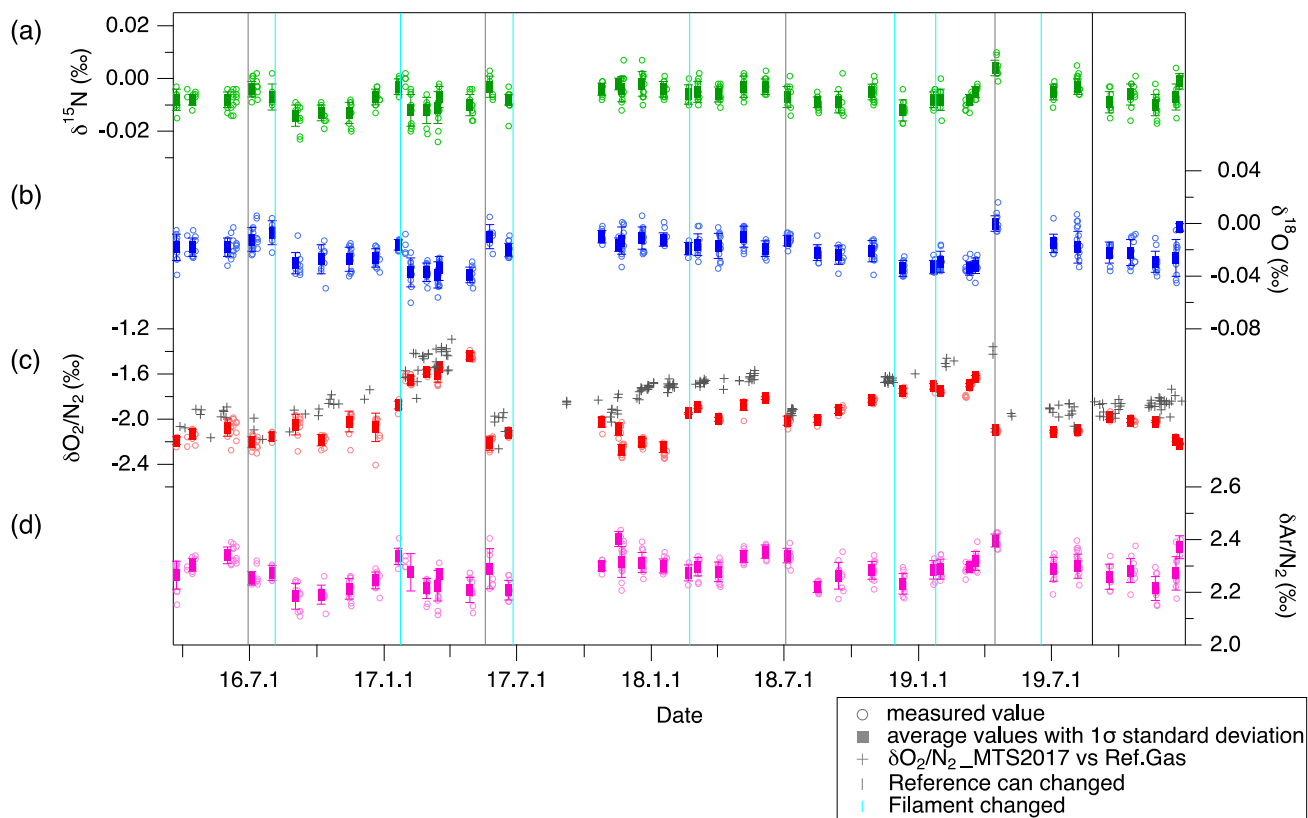
935

940

Figure 6: Change of $\delta O_2/N_2$ by wet extraction and overnight storage. Dashed line represents exponential fit to the data ($\Delta\delta_{\text{extraction, O2/N2}}$ = -0.55362 exp(-0.31606 $\times$ V) + -0.078802).

945

Figure 7: Atmospheric composition measured against reference gas for (a) $\delta_{15}N$, (b) $\delta_{18}O$, (c) $\delta O_2/N_2$, and (d) $\delta Ar/N_2$. Open markers represent individual data points, whereas filled markers represent the means of values measured within several days (error bars are one standard deviations). Grey plus (+) markers in (d) represent estimated $\delta O_2/N_2$ of MTS-2017 against reference gas through the measurements of STD-A against the reference gas, assuming that $\delta O_2/N_2$ of STD-A has not changed. Vertical grey lines indicate the timing of replacements of reference can, and vertical light blue lines indicate the timing of filament replacements.

950
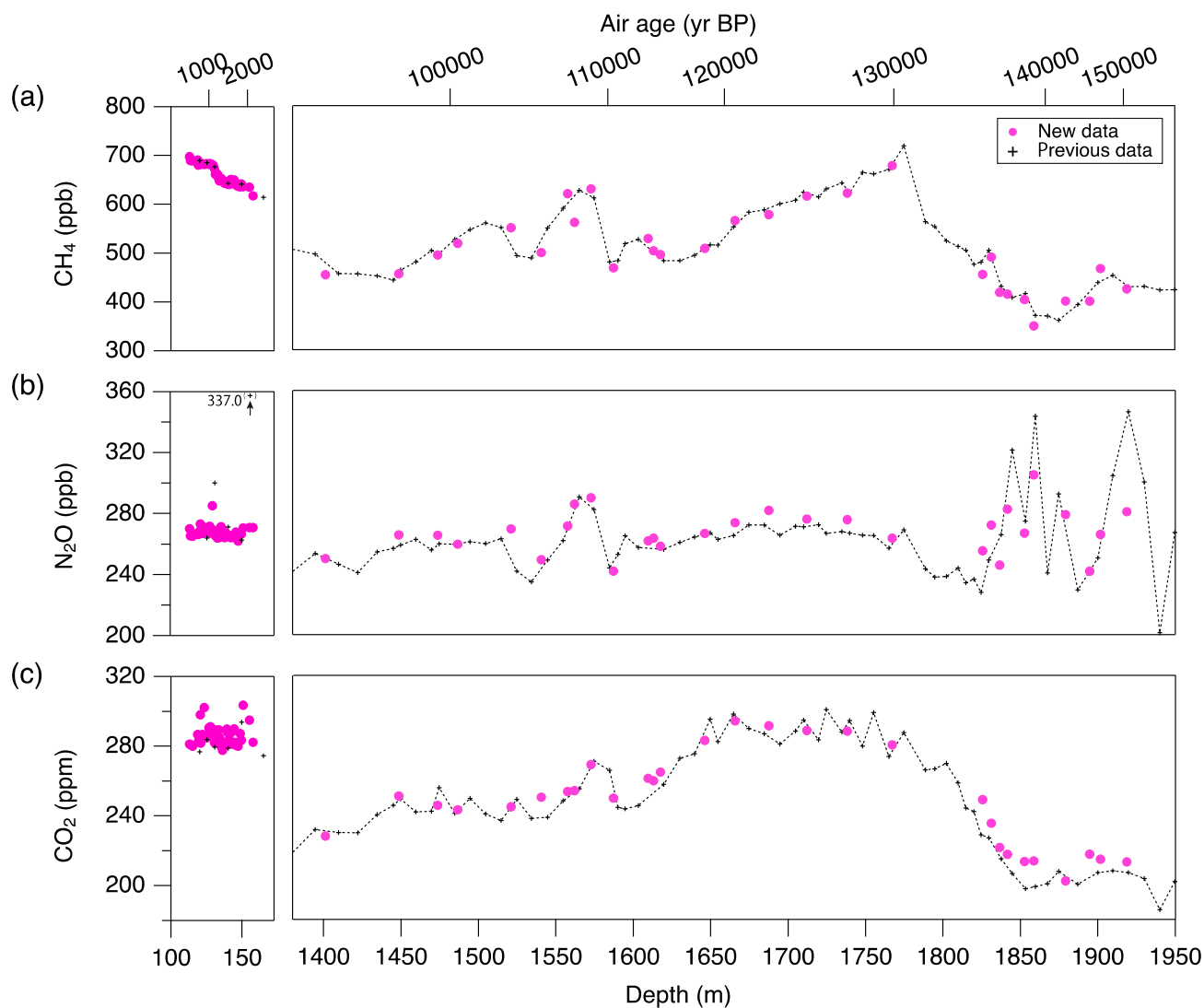
Figure 8: CH_4, N_2O and CO_2 concentrations of the Dome Fuji ice core, and comparison with previous records from the same core (Kawamura, 2000 and Kawamura et al., 2007).

955

960

Atmospheric
Measurement
Techniques
Discussions
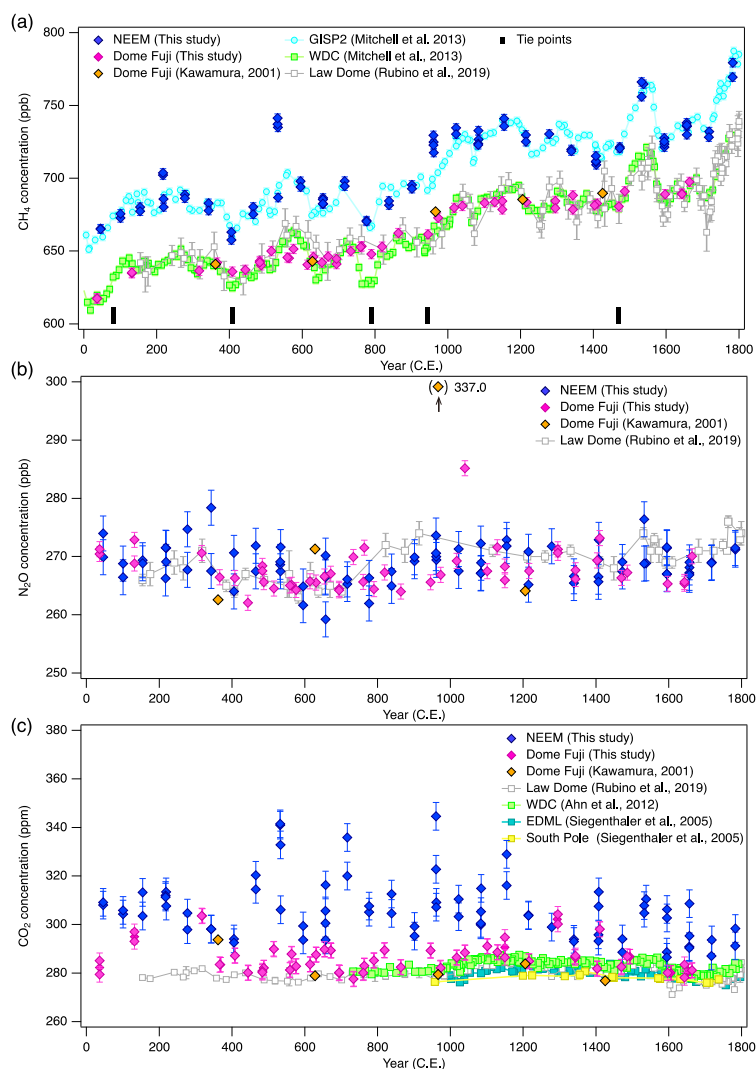
Figure 9: (a) CH_4, (b) N_2O and (c) CO_2 concentrations for 0 – 1800 C.E. from the DF and NEEM ice cores measured with our new method, and the comparison with published records from other groups (Ahn et al., 2012; Kawamura, 2001; Kawamura et al., 2007; Mitchell et al., 2013; Rubino et al., 2019; Siegenthaler et al., 2005). The DF data is placed on the WDC05A chronology by placing 5 tie points between the CH_4 variations of the DF and WD cores (thick tick marks at the bottom of (a)), and all the other data are placed on the respective (published) time scales. Details are summarized in Table A1.
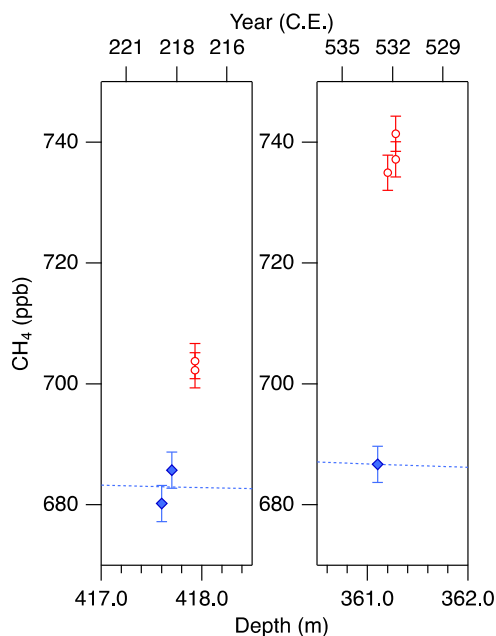
970

Figure 10: Detailed views of individual CH4 data for the abrupt (non-atmospheric) increases in the NEEM core at ~418 and 361 m. Data shown in blue agree with the GISP2 data, and those in red are unrealistically high (interpreted as natural artefacts). The dotted line (blue) connects the blue markers (mean of two data for 417 m and one data for 361 m) with their neighbouring data points.

975
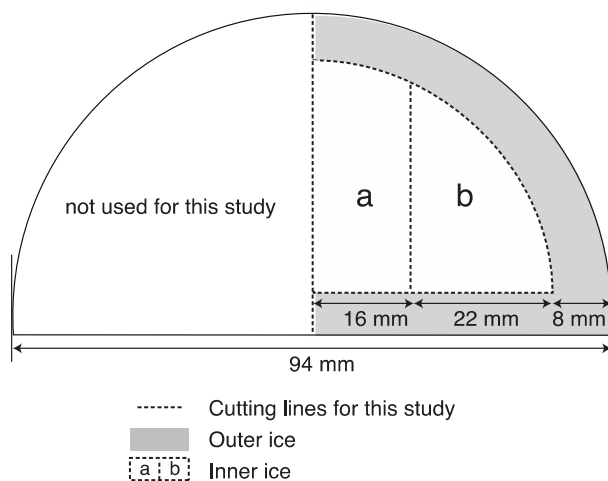
Figure: 11: Typical cross-sectional cutting plan of the DF core for duplicate measurements and outer-inner comparisons for mass spectrometer analyses. The sample length is ~12 cm. The original outer surface (black line) has been exposed to the atmosphere for ~20 years. Dotted lines indicate the boundaries between "a," "b," and "outer" pieces. For single (non-duplicate) measurements, "a" piece is not cut.

980
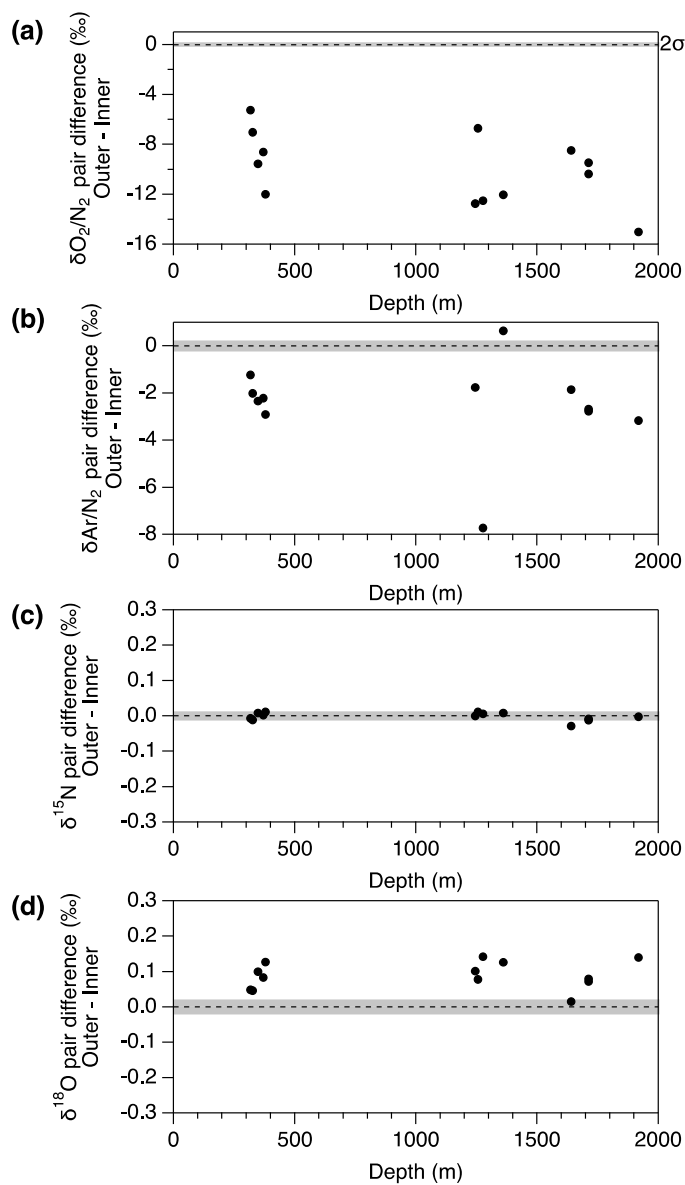
Figure 12: Difference between outer ice and inner ice for (a) $\delta O_2/N_2$, (b) $\delta Ar/N_2$, (c) $\delta^{15}N$, and (d) $\delta^{18}O$. Grey shadings indicate the estimated 2σ uncertainty for clathrate ice (from pooled standard deviations of duplicates with > 8 mm of outer removal).
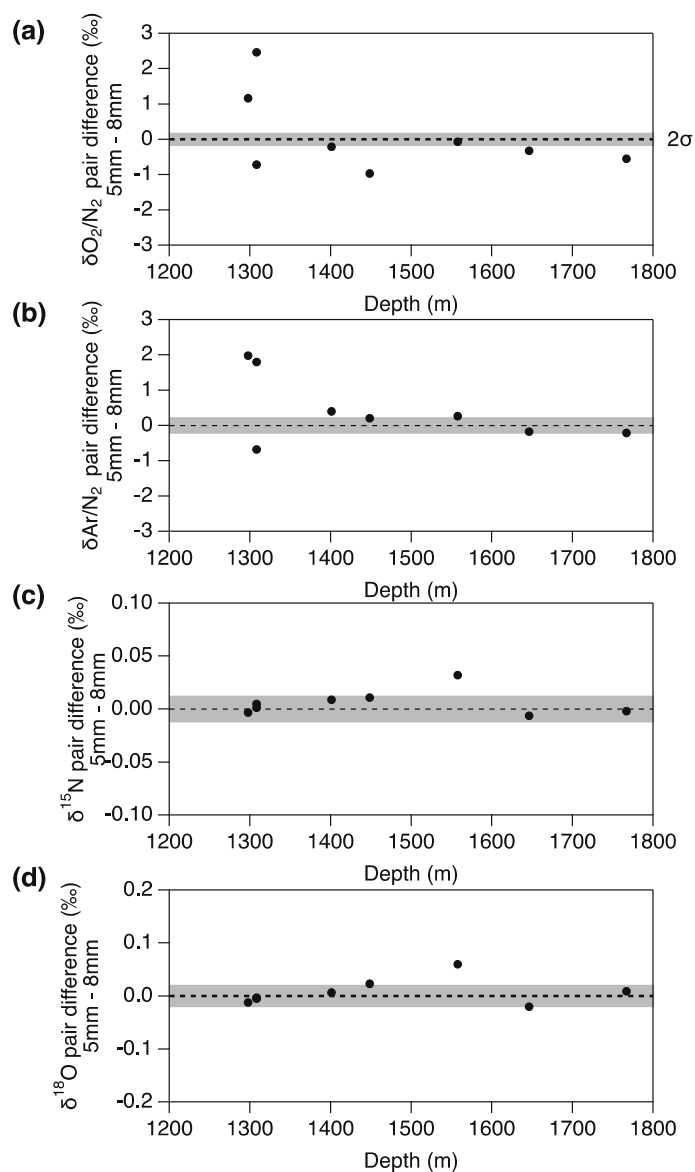
Figure 13: Pair difference between the two inner ice with the thickness of outer removal of 5 mm and 8 mm for (a) $\delta O_2/N_2$, (b) $\delta Ar/N_2$, (c) $\delta^{15}N$, and (d) $\delta^{18}O$. Grey shadings indicate the estimated 2σ uncertainty for clathrate ice (from pooled standard deviations of duplicates with > 8 mm of outer removal).
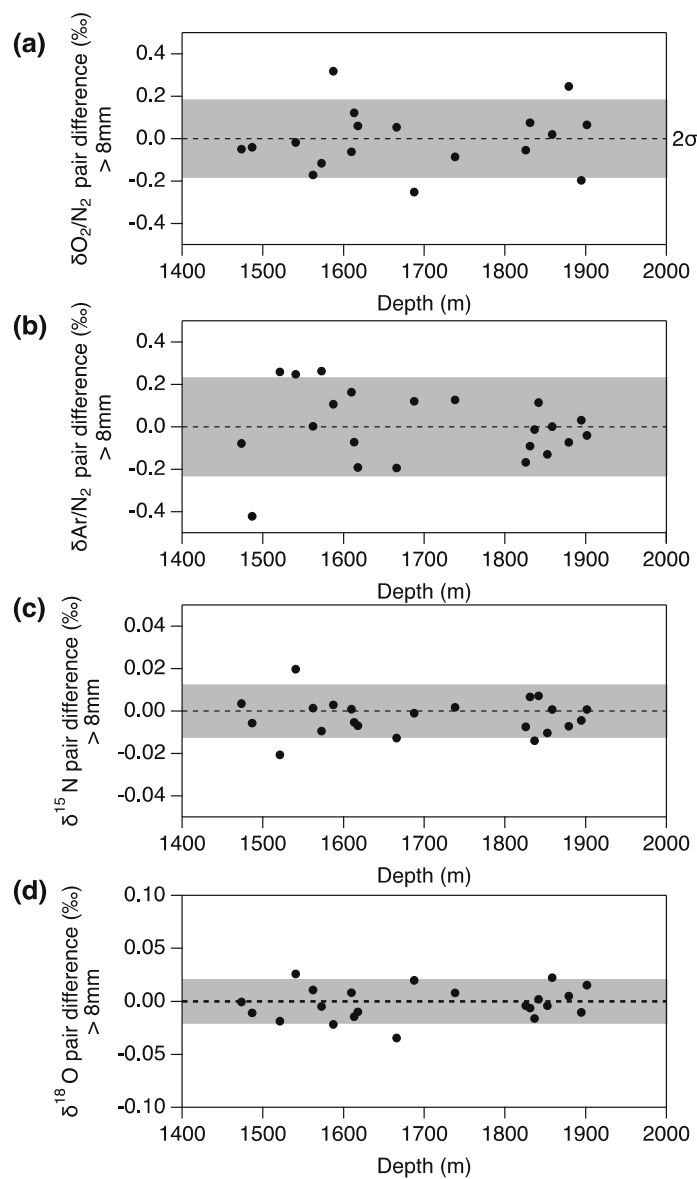
Figure 14: Pair difference between the two inner ice with the thickness of outer removal of > 8 mm for (a) $\delta O_2/N_2$, (b) $\delta Ar/N_2$, (c) $\delta^{15}N$, and (d) $\delta^{18}O$. Grey shadings indicate the estimated 2σ uncertainty for clathrate ice (from pooled standard deviations of duplicates with > 8 mm of outer removal).
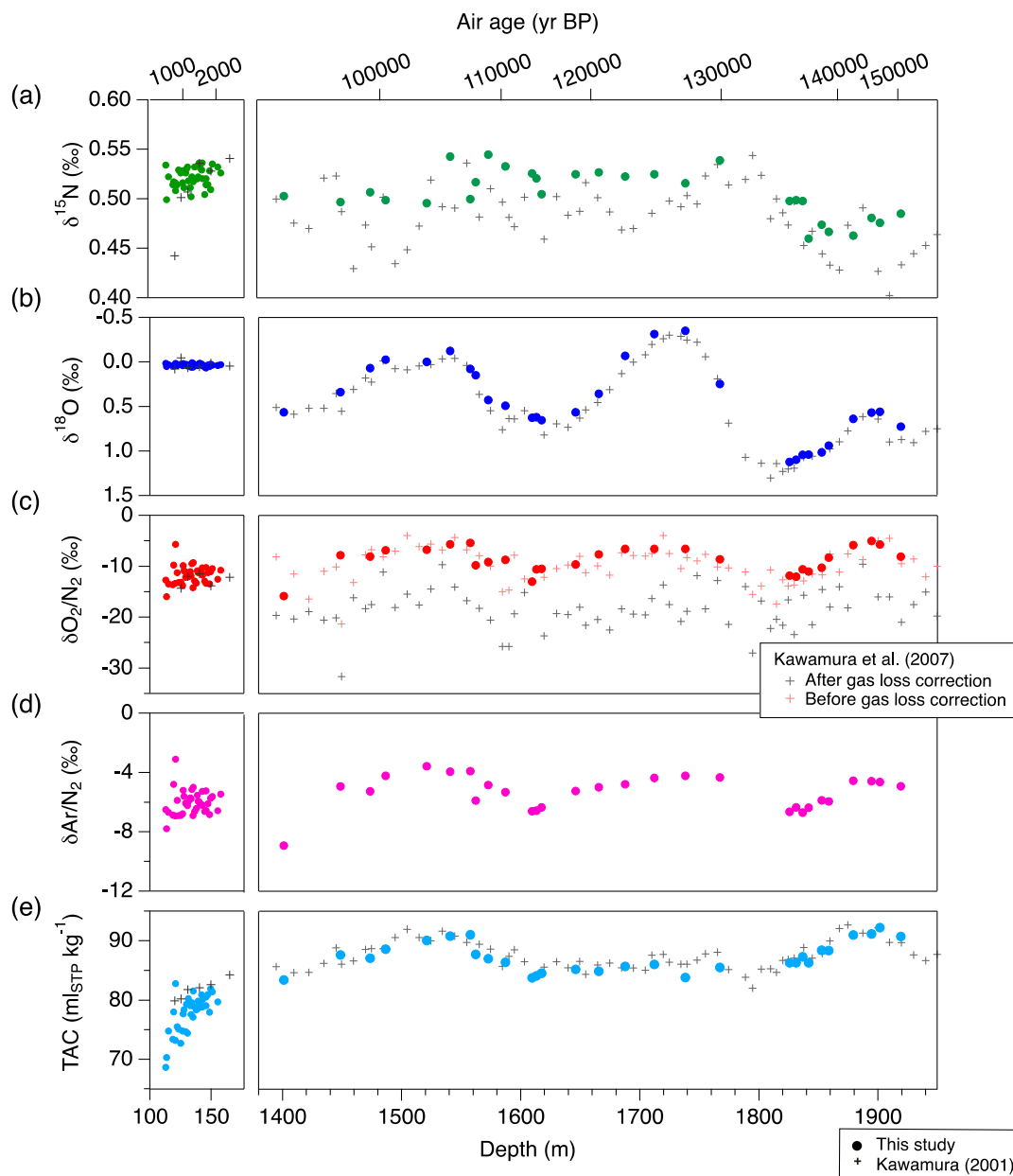
Figure15: The DF records of mass spectrometer measurements and TAC from this study (filled markers), and comparison with previous records from the same core (crosses connected with dotted lines, Kawamura, 2000; Kawamura et al., 2007). (a) δ^{15}N, (b) δ^{18}O, (c) $\delta O_2/N_2$, (d) $\delta Ar/N_2$, and (e) TAC. For the previous $\delta O_2/N_2$ records in the right panel of (c), both raw data (black) and corrected data for gas-loss fractionation during core storage at -25 °C (red) are shown.

Atmospheric
Measurement
Techniques
Discussions

Tables

1005   **Table 1: Settings of gas chromatographs.**

	GC1		GC2
	CH$_4$	CO$_2$	N$_2$O
Carrier gas	N$_2$, 10 ml min^{-1}		He, 7 ml min^{-1}
Sample loop volume	0.5 ml		0.5 ml
Oven temperature	30 ˚C		30 ˚C
Column	GS-CarbonPLOT		HP-PLOT/Q
Length	30 m		30 m
Internal diameter	0.53 mm		0.53 mm
Film thickness	3 μm		40 μm
Ni-catalyst temperature	None	400 ˚C	None
Detector	FID	FID	ECD
Temperature	200 ˚C	200 ˚C	325 ˚C
H$_2$ flow rate	35 ml min^{-1}	40 ml min^{-1}	None
Air flow rate	400 ml min^{-1}	400 ml min^{-1}	None
Make-up gas	N$_2$, 20 ml min^{-1}	N$_2$, 20 ml min^{-1}	Ar+CH$_4$ (5%), 10 ml min^{-1}

Table: 2: Standard gases.

	STD 1	STD 2	STD 3	STD 4	STD 5	STD A	STD B	scale
Cylinder ID	CQB09303	CQB12403	CQB09309	CQB07938	CQB09336	CRC00059	CRC00057	
CH$_4$ [ppb]	255.3	430.9	609.9	796.2	968.8	526.7	720.2	TU-2008
N$_2$O [ppb]	186.2	222.9	259.7	298.1	317.9	241.3	273.2	TU-2006
CO$_2$ [ppm]	169.79	209.25	249.64	289.37	330.71	229.04	269.21	TU-2008

1010

1015

Atmospheric
Measurement
Techniques
Discussions
EGU
Open Access

Table 3: Collector configurations of the mass spectrometer.

Mass	Slit width (mm)	Resistor (Ω)	Typical ion current (A)
28	2.0	3×10^8	2×10^{-8}
29	3.8	3×10^{10}	1×10^{-10}
32	3.8	1×10^9	4×10^{-9}
33	1.4	1×10^{12}	3×10^{-12}
34	3.8	3×10^{11}	2×10^{-11}
36	2.0	1×10^{12}	1×10^{-12}
38	1.4	1×10^{12}	2×10^{-13}
40	2.0	3×10^9	3×10^{-10}
44	2.4	1×10^{10}	4×10^{-12}

1020

Table 4: Test results using a standard gas (STD-A) for greenhouse gases.

		CH_4 (ppb)	N_2O (ppb)	CO_2 (ppm)	n
Sample tubes	Average	+0.8	+1.3	+0.1	25
(overnight storing)	Std. dev.	2.1	2.1	1.1	
Test tubes	Average	+0.7	+0.9	-0.2	17
(immediate measurement)	Std. dev.	2.2	1.0	0.1	
Extraction line	Average	+1.5	+0.8	+1.1	9
(mimicking ice core extraction)	Std. dev.	1.6	1.3	0.7	

Values are differences from the calibrated concentrations of the STD-A cylinder (Table 3)

1025

Table 5: Composition of STD-A for mass spectrometer measurements.

	$\delta^{15}N$ (‰)	$\delta^{18}O$ (‰)	$\delta O_2/N_2$ (‰)	$\delta Ar/N_2$ (‰)	n
Mean	-0.018	0.002	2.595	-2.171	214 (18 for $\delta O_2/N_2$)
Std. error	<0.001	<0.001	0.008	0.006	

$\delta O_2/N_2$ is determined in Jul. 2019 against the 2017 annual mean $\delta O_2/N_2$ over Minamitorishima island provided by AIST. Other ratios are

1030   determined against outside air sampled monthly at NIPR over Feb. 2016 – Dec. 2019.

Atmospheric
Measurement
Techniques
Discussions

Table 6: Age control points for the DF core from CH$_4$ matching to the WDC core (0 – 1800 C.E.)

DF depth (m)	WDC05A age (C.E.)	Approximate 1σ error [a] (year)
119.23	1470	42
131.29	945	42
134.17	790	33
148.65	408	41
156.515	80	44

[a] estimated as the half of the mean age intervals from the tie point to the neighbouring CH$_4$ data points (uncertainty of WDC05A itself is also considered).

1035

Table 7: Pooled standard deviations for the NEEM and Dome Fuji ice cores.

	CH$_4$ (ppb)	N$_2$O (ppb)	CO$_2$ (ppm)	TAC (ml$_{STP}$ kg^{-1})	Number of pairs	δ^{15}N (‰)	δ^{18}O (‰)	δO$_2$/N$_2$ (‰)	δAr/N$_2$ (‰)	Number of pairs
NEEM (bubble)	2.9	3.0	5.5		25	0.006	0.008	0.775	0.450	23
DF (bubble)	3.2	1.3	3.2	0.66	8	0.009	0.018	0.236	0.120	8
DF (clathrate)	3.2	2.2	3.1	0.67	29	0.006	0.010	0.089	0.115	22

1040

Atmospheric
Measurement
Techniques
Discussions
Open Access
EGU

Appendix A: Comparison with other available records

Table A1: Ice cores and time scales shown in this study.

	Ice core	Reference	Offset (ppb)	Time scale
CH$_4$	NEEM	This study		GICC05 (Rasmussen et al., 2013)
	Dome Fuji	This study		WDC05A (Mitchell et al., 2013; Mitchell et al., 2011)
	Dome Fuji	Kawamura (2001)		WDC05A (Mitchell et al., 2013; Mitchell et al., 2011)
	GISP2	Mitchell et al. (2013)		WDC05A (Mitchell et al., 2013; Mitchell et al., 2011)
	GISP2	Brook (2009)		WDC05A (Mitchell et al., 2013; Mitchell et al., 2011)
	GRIP	Blunier et al. (1995); Chappellaz et al. (1997); Chappellaz et al. (1993)	+23.84[a]	GICC05 (Rasmussen et al., 2014; Seierstad et al., 2014)
	NGRIP	Beck et al. (2018)	+6.15[a]	GICC05 (Rasmussen et al., 2014; Seierstad et al., 2014)
	WAIS Divide	Mitchell et al. (2013)		WDC05A (Mitchell et al., 2013; Mitchell et al., 2011)
	Law Dome	Rubino et al. (2019)		Rubino et al. (2019)
	Dome C	Flückiger et al. (2002)	+10.38[a]	Beck et al. (2018)
	EDML	Schilt et al. (2010)	+1.52[a]	Beck et al. (2018)
	TALDAICE	Beck et al. (2018)	+6.15[a]	Beck et al. (2018)
	TALDAICE	Bock et al. (2017)	+6.15[a]	Beck et al. (2018)
	TALDAICE	Schilt et al. (2010)	+4.06[a]	Beck et al. (2018)
	Siple Dome	Brook (2009)		Beck et al. (2018)
N$_2$O	NEEM	This study		GICC05 (Rasmussen et al., 2013)
	Dome Fuji	This study		WDC05A (Mitchell et al., 2013; Mitchell et al., 2011)
	Dome Fuji	Kawamura (2001)		WDC05A (Mitchell et al., 2013; Mitchell et al., 2011)
	EURO core	Flückiger et al. (1999)		Flückiger et al. (1999)
	GRIP	Flückiger et al. (1999)		GICC05 (Rasmussen et al., 2014; Seierstad et al., 2014)
	GISP2	Sowers et al. (2003)		WDC05A (Mitchell et al., 2013; Mitchell et al., 2011)
	Law Dome	Rubino et al. (2019)		Rubino et al. (2019)
	H15	Matchida et al. (1995)		Machida et al. (1995)
	EDC	Schilt et al. (2010)		Beck et al. (2018)
	TALDICE	Schilt et al. (2010)		Beck et al. (2018)
	EDML	Schilt et al. (2010)		Beck et al. (2018)
	NEEM	Prokopiou et al. (2018)		GICC05 (Rasmussen et al., 2013)
CO$_2$	NEEM	This study		GICC05 (Rasmussen et al., 2013)
	Dome Fuji	This study		WDC05A (Mitchell et al., 2013; Mitchell et al., 2011)
	Dome Fuji	Kawamura et al. (2007)		WDC05A (Mitchell et al., 2013; Mitchell et al., 2011)
	Law Dome	Rubino et al. (2019)		Rubino et al. (2019)
	WDC	Ahn et al. (2012)		Ahn et al. (2012)
	EDML	Siegenthaler et al. (2005)		Siegenthaler et al. (2005)
	South Pole	Siegenthaler et al. (2005)		Siegenthaler et al. (2005)

1045   [a] Offset correction was made to CH$_4$ concentrations by following Beck et al. (2018).

Atmospheric
Measurement
Techniques
Open Access

Discussions
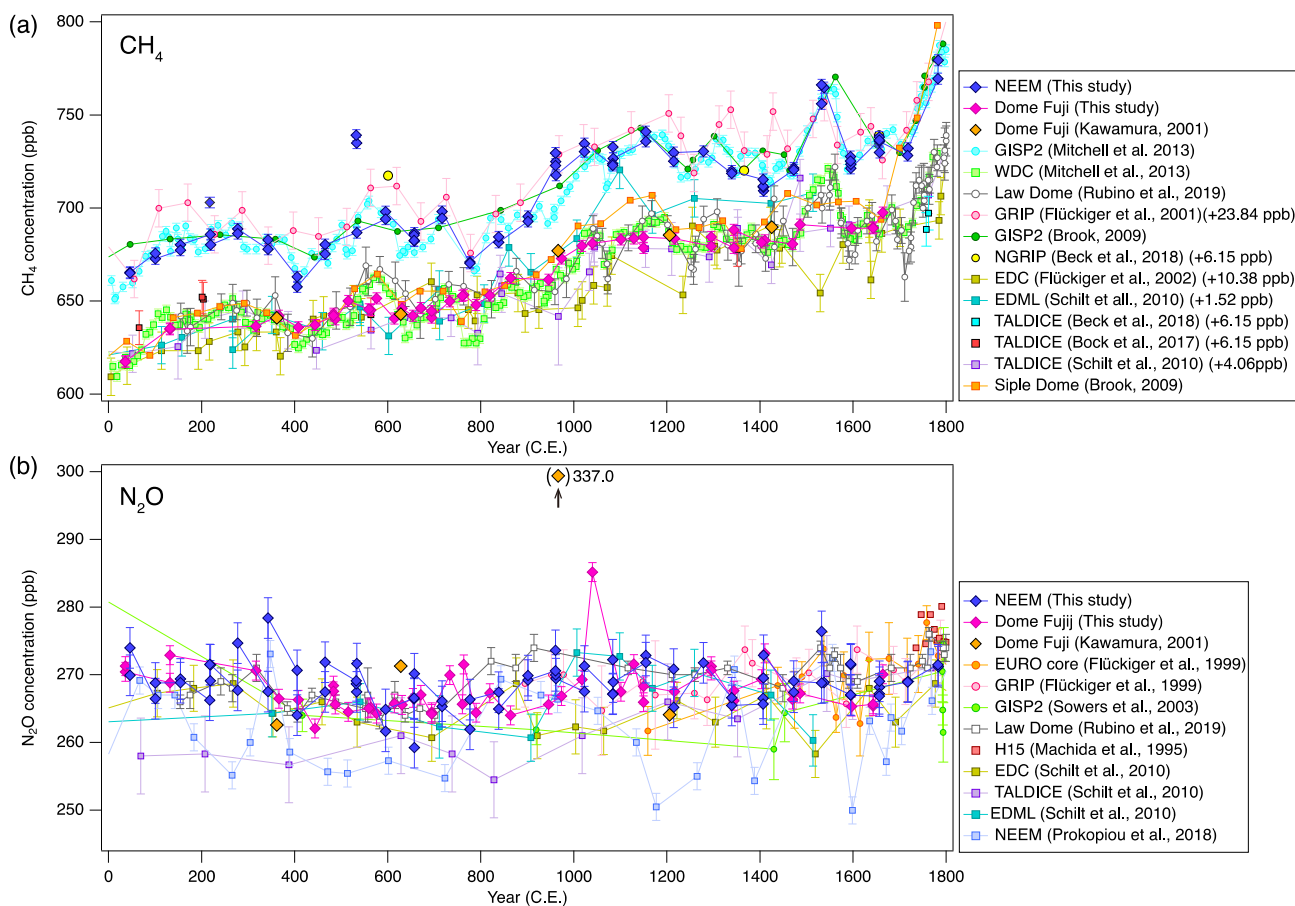
Figure A1: (a) CH$_4$ and (b) N$_2$O concentrations for 0 – 1800 C.E. from the DF and NEEM ice cores measured with our new method, and the comparison with published records from other groups (Beck et al., 2018; Bock et al., 2017; Brook, 2009; Flückiger et al., 1999; Flückiger et al., 2002; Kawamura, 2001; Machida et al., 1995; Mitchell et al., 2013; Prokopiou et al., 2018; Rubino et al., 2019; Schilt et al., 2010; Sowers et al., 2003). The DF data is placed on the WDC05A chronology (see Fig. 9), and all the other data are placed on the respective (published) time scales (details are summarized in Table A1). The GRIP, NGRIP, EDC, EDML, and TALDICE data are corrected for systematic offsets relative to the WDC data, as reported by Beck et al. (2018).

1050

1055